2-2-3. Results of semi-detailed survey

1. Provisional resistivity and IP cross sections of semi-detailed survey

The lines were determined in semi-detailed survey from IP anomalous zones which were detected by reconnaissance survey of the lines C, L, O, X, Y and Za which were presumed to have detected IP anomalies shown in Fig.II-2-1. The electrode separation survey 100m to detect the source of IP anomalies of the shallow IP anomalies.

Resistivity and IP cross section with the result of the semi-detailed survey are shown in Fig.II-2-7 to Fig.II-2-12.

The Binge site

C and Cs line(Fig.II-2-7)

Cs line was set up 150m south of C line.

Tendencies of low resistivity/low IP and high resistivity/high IP are shown on each line, and all the IP patterns correlate.

The IP anomalous pattern of the eastern side of Cs line is weak.

The Greenfields site

Ln, Lc, L and Ls line(Fig.II-2-8)

The line L was extended 600m to the east.The line Ln and the line Ls were set up 200m to the north and 400m to the south of the line L,
respectively. The line Lc is on the line L, and the electrodes separation is 100m.

The distribution of IP anomalies of the eastern part by the extension of line L and setting 100m electrodes separation was analysed. Comparing the IP anomaly patterns by 200m and 100m electrodes separation in the same depth, the IP anomaly pattern by 100m electrodes separation shows more complex patterns than by 200m electrodes separation. This means that 100m electrodes separation shows distinct sensitivity for IP anomaly. The IP anomaly shows complex shape from the shallow part to the deep part under the stations No.12 to No.22.

An indistinct IP anomaly(6.8mV) was detected under the stations No.7 to No.10 in Ln line.

An indistinct IP anomaly(5.2mV) was detected near the surface of the stations No.8 to No.12 in Ls line. The anomaly is less distinct than in the Ln survey line.

Za line(Fig.II-2-9)

This line was extended 1km to the west.

The IP anomalous zone is widely distributed in the western side. The anomalous pattern shows distinct shape which widens towards the deeper part. The IP anomaly which is located in the station No.0 corresponds to arkose. The eastern part of the station No.4 is the distribution area of the basement granite.

The Inyati site

On, O, Os, Osc, Oss line(Fig.II-2-10)

Osc survey line with 100m electrodes separation was set up on the Os survey line.

On survey line, Os survey line and Oss survey line were set up 400m north, 200m south and 250m south of O survey line, respectively.

The IP anomaly of the anomalous zone in On line which is the same pattern in O section is weaker than that of O section.

There is distinct IP pattern of the shallow part in Os and Osc section.

The IP anomaly pattern by 100m electrodes separation shows more clear pattern near the surface of the station of No.8 to No.9 in Osc line.

There are IP anomalies in Os and Oss lines however, it suggests that IP anomaly decreases in Oss line which is the south of Os section.

The Angwa site

Xn, X, Xs line(Fig.II-2-11)

Xn and Xs survey lines were set 150m north and 150m south of X survey line, respectively.

All the lines show the tendency of high resistivity and high IP anomaly.

The Ip anomalies are distributed in the west end of Xn, X line, and centre part of in Xs line, respectively.

The Ip anomalies in all the lines are recognised in the area comprising arkose.

Yn, Y, Ys line(Fig.II-2-12)

Yn and Ys survey lines were set 150m north and 150m south of Y survey line, respectively.

All the lines show the tendency of high resistivity and high IP anomaly.

The distinct IP anomaly of the deeper part are distributed in the station No.10 to No.14 in Ys line.

The IP anomaly in Ys section is more distinct than that in Y section. All the anomalies are recognised in the comprising area of arkose.

The characteristics of IP anomalies are summarised in Table II-2-5.

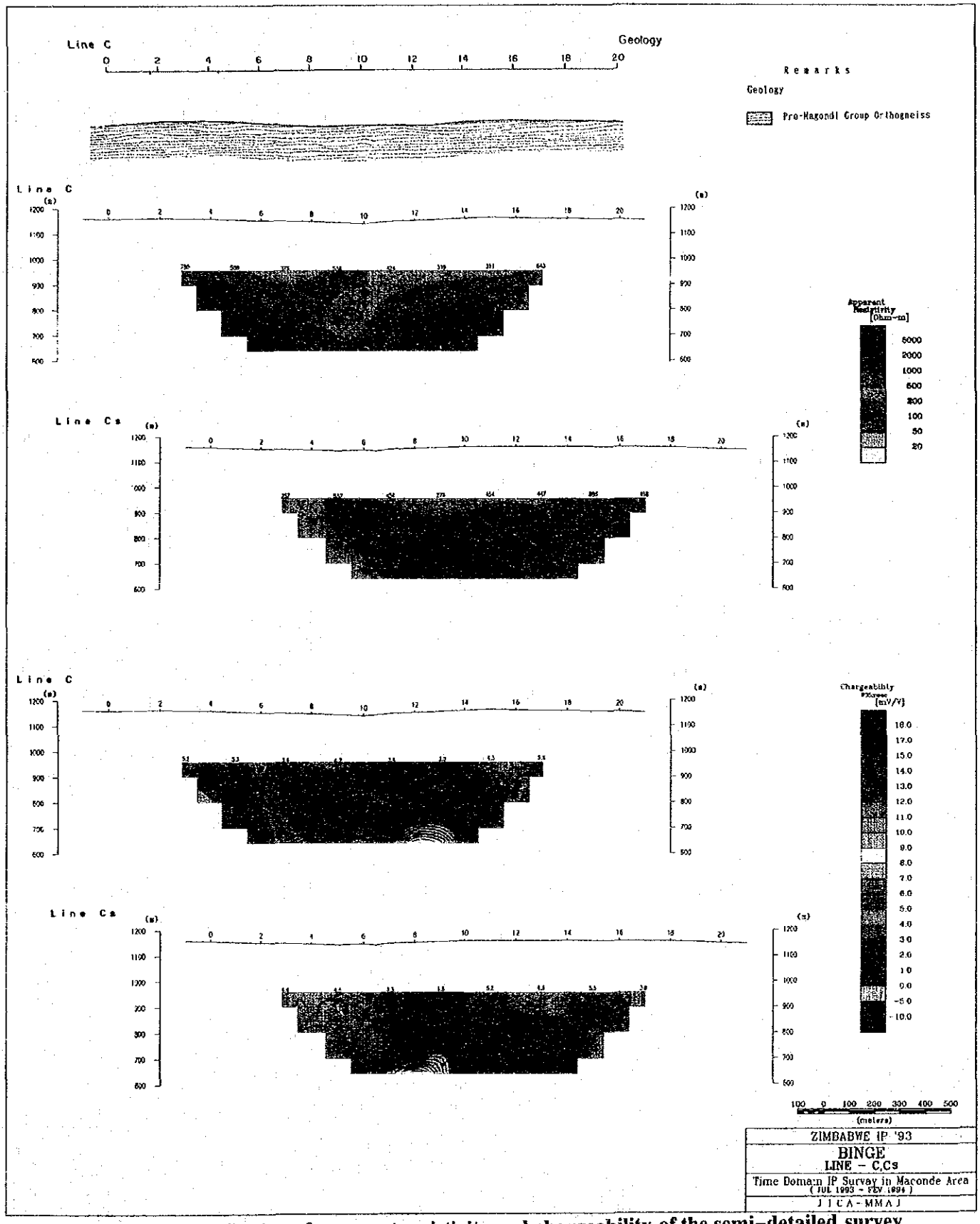

Fig.II-2-7 Section of apparent resistivity and chargeability of the semi-detailed survey (C,Cs line)

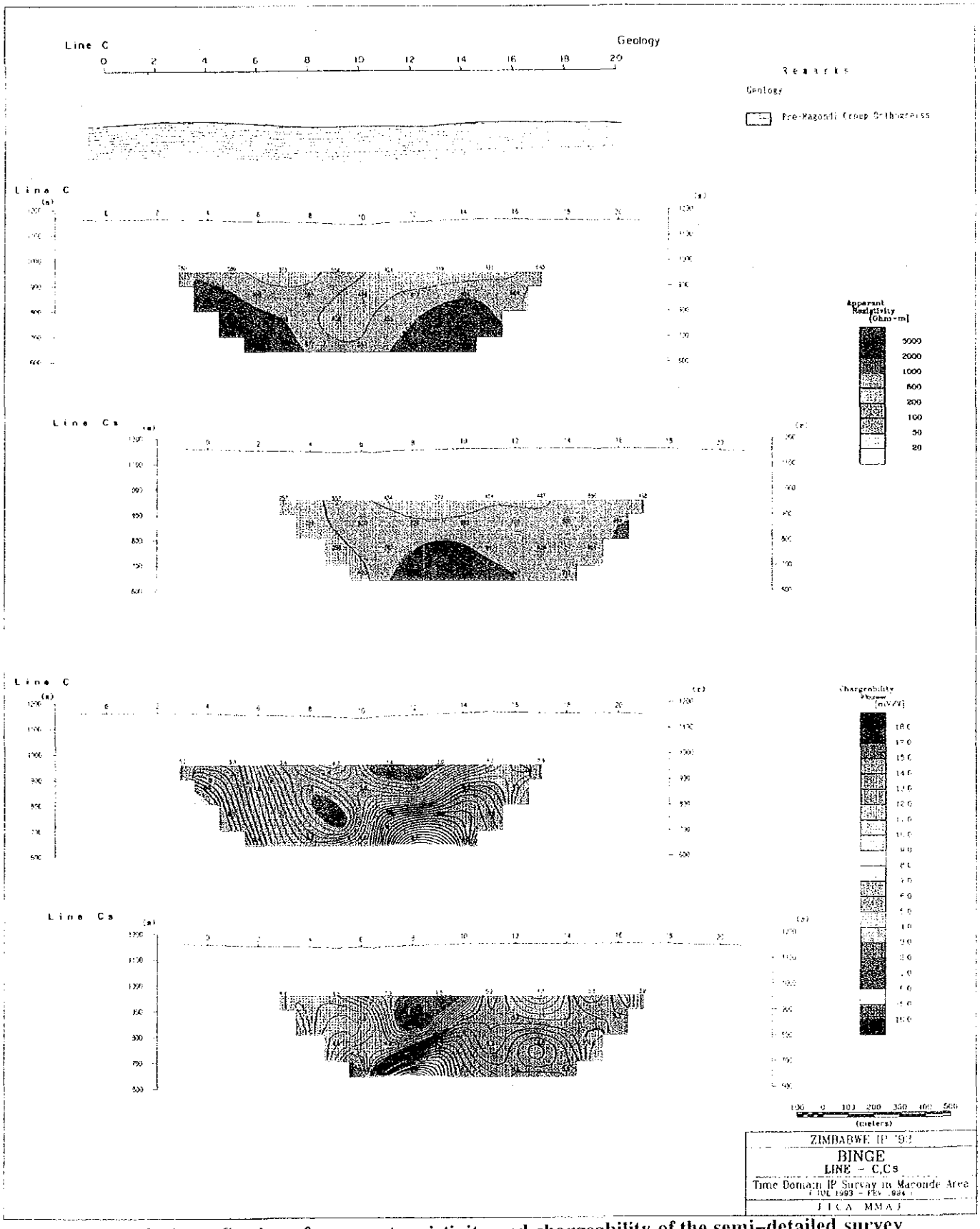

Fig.II-2-7 Section of apparent resistivity and chargeability of the semi-detailed survey (C,Cs line)

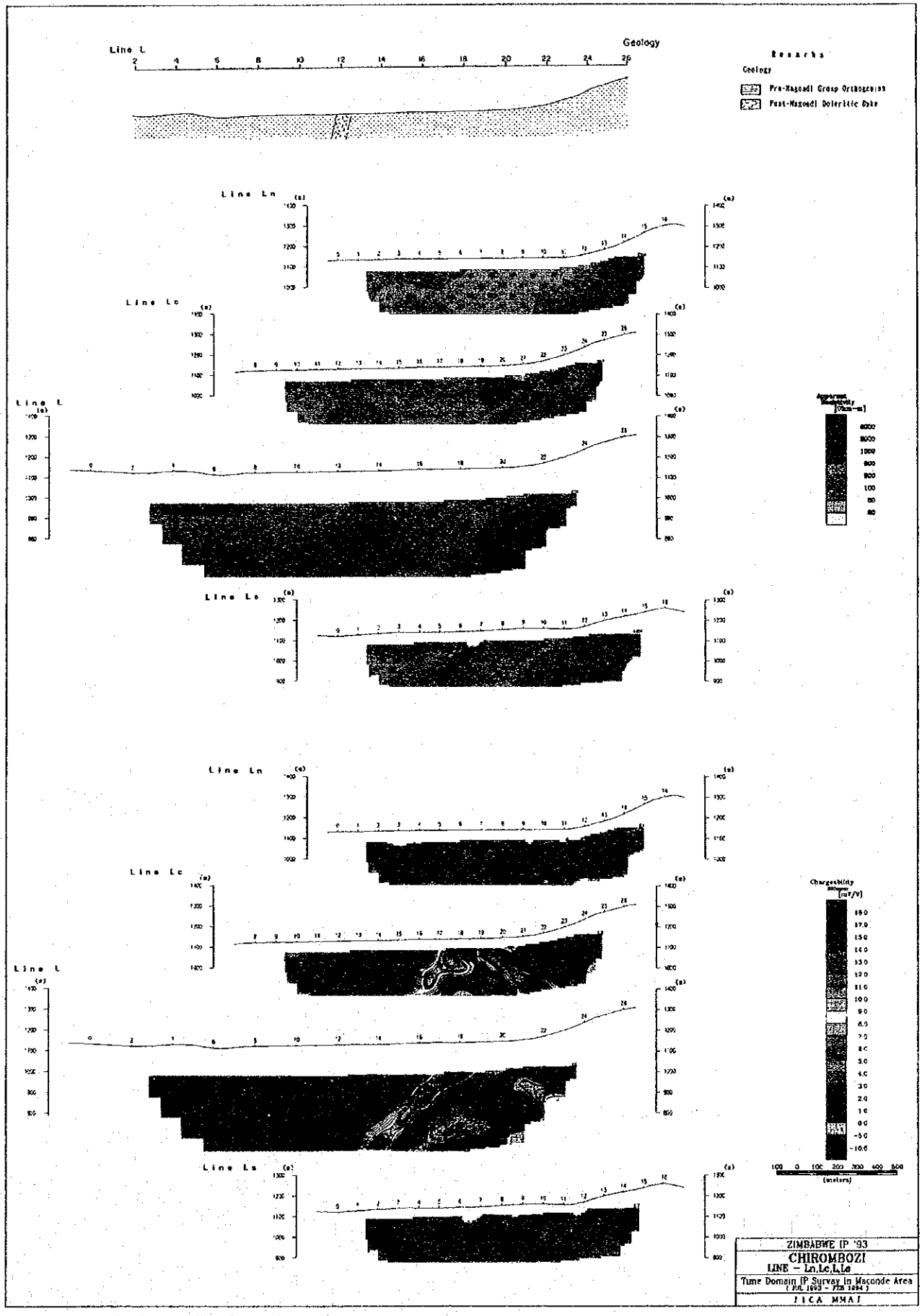

Fig.II–2–8 Section of apparent resistivity of and chargeability the semi–detailed survey (Ln,Lc,L,Ls line)

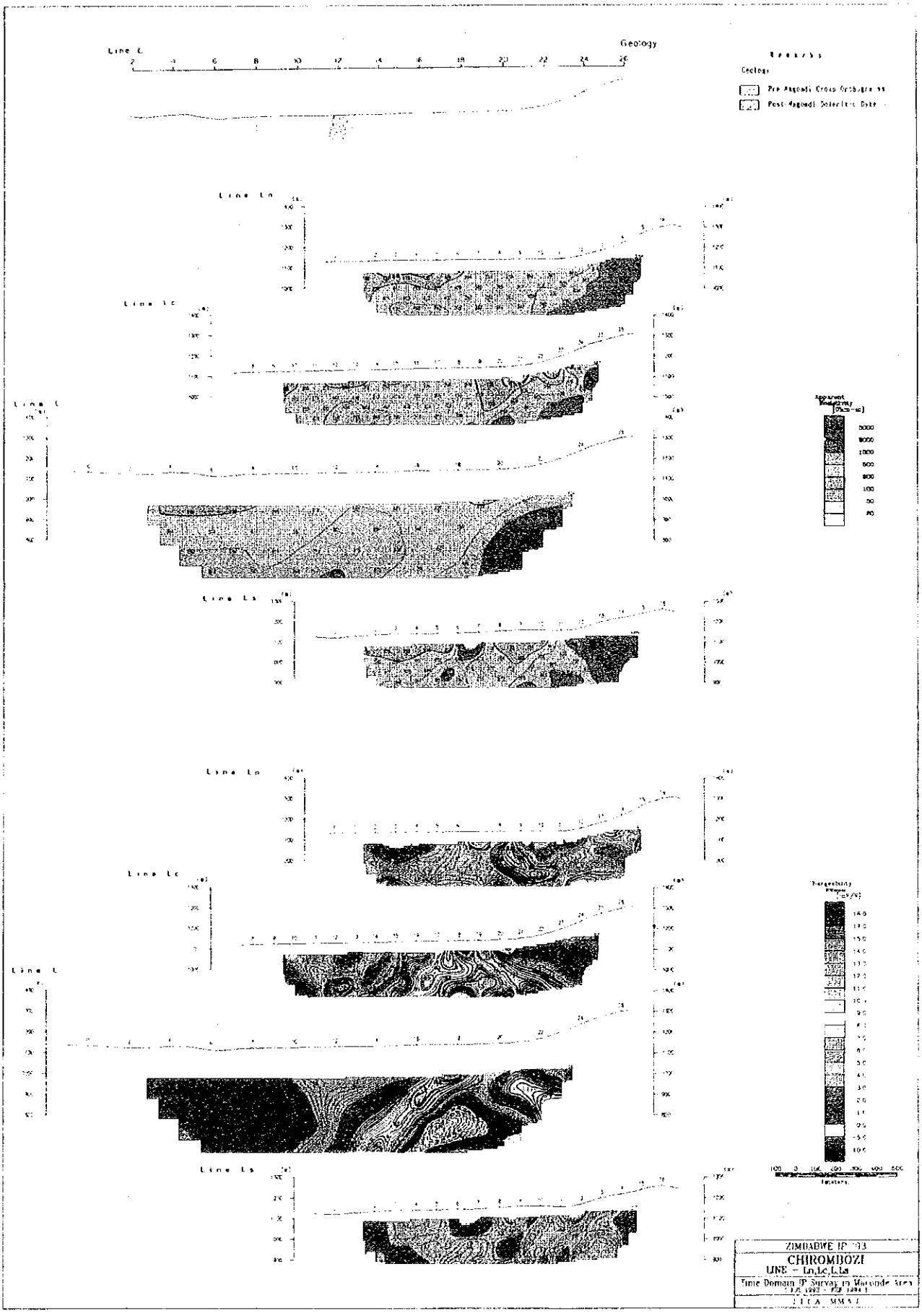

Fig.II-2-8 Section of apparent resistivity of and chargeability the semi-detailed survey (Ln,Lc,L,Ls line)

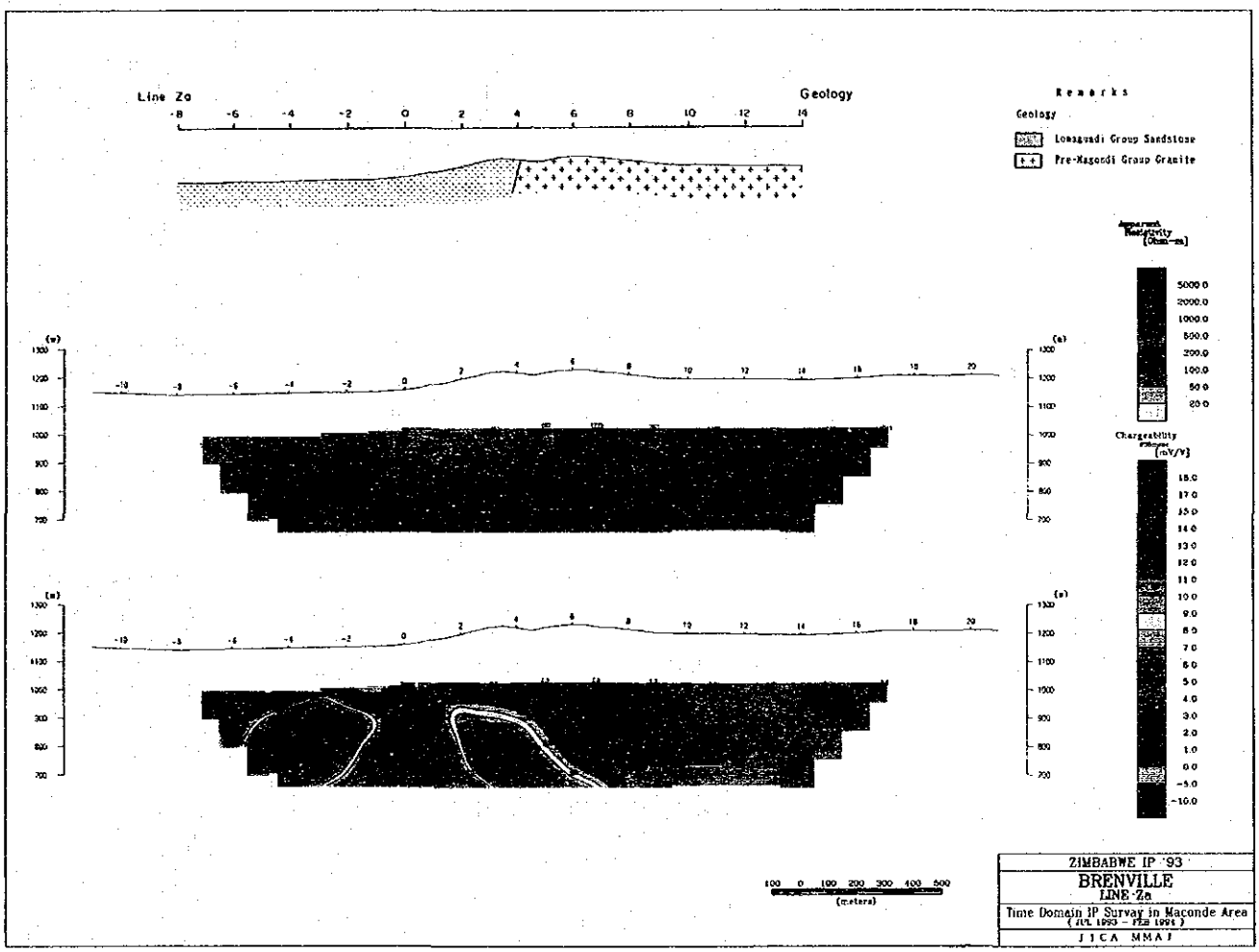

Fig.II-2-9 Section of apparent resistivity and chargeability of the semi-detailed survey (Za line)

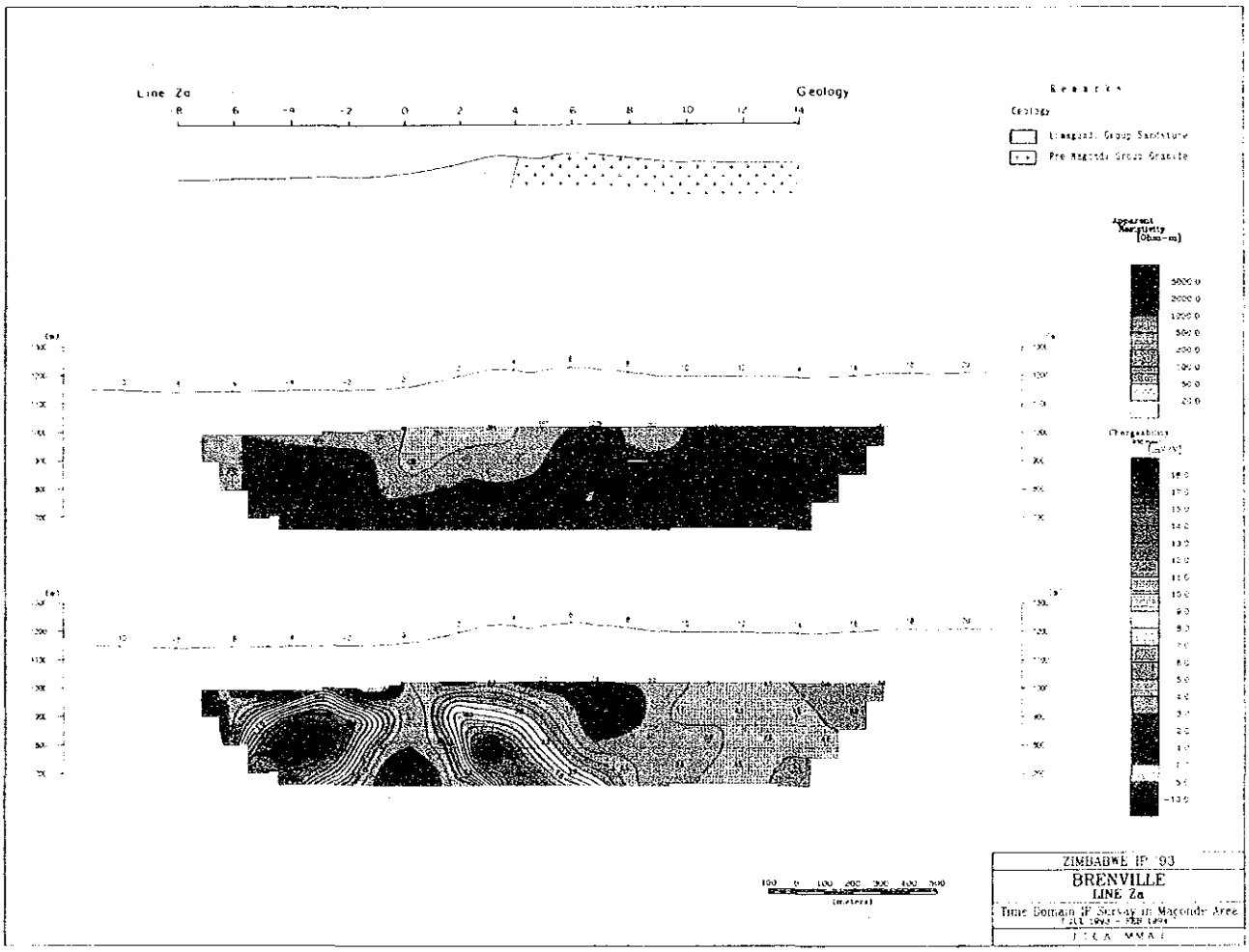

Fig.II-2-9 Section of apparent resistivity and chargeability of the semi-detailed survey (Za line)

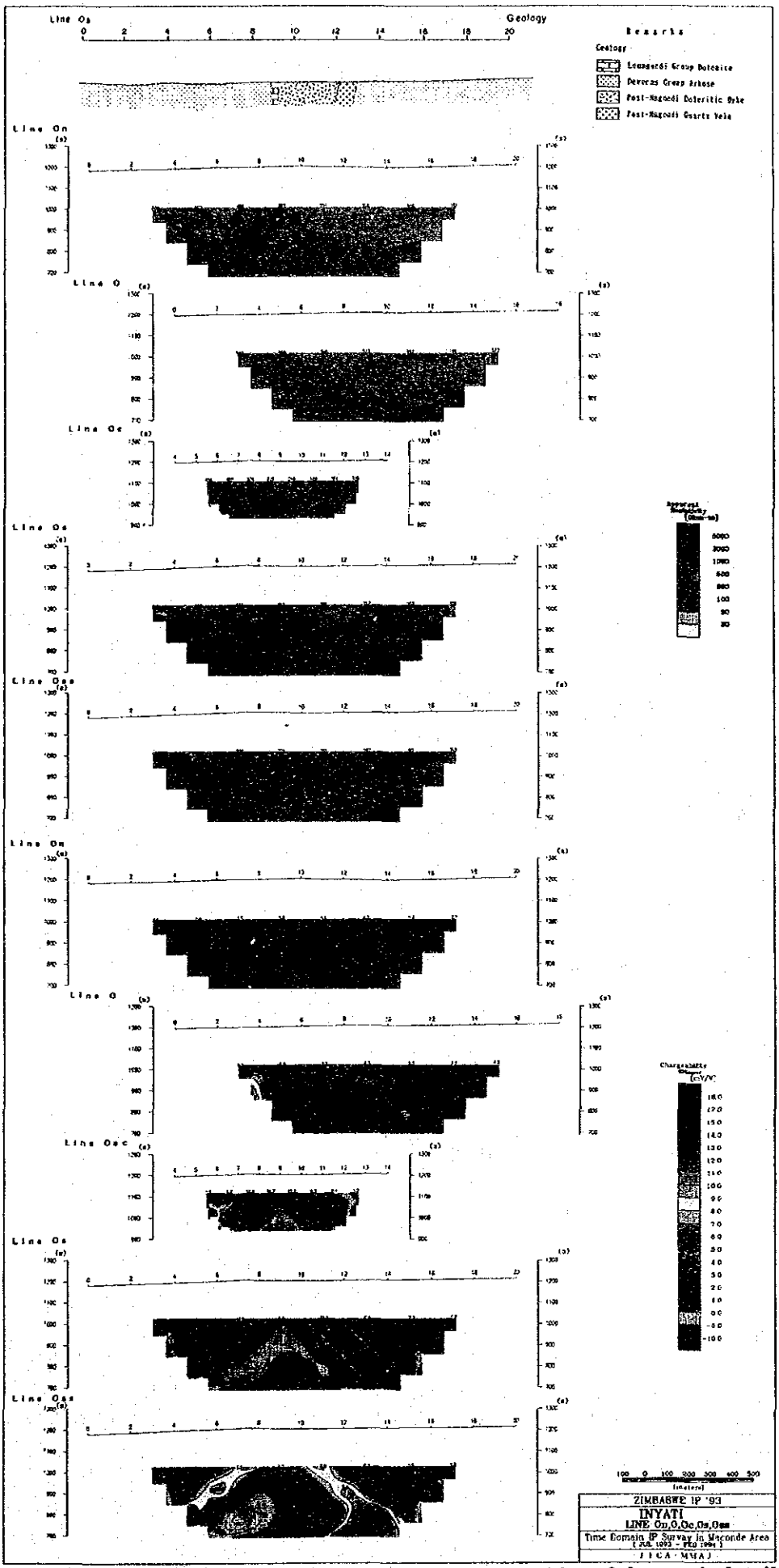

Fig.II–2–10 Section of apparent resistivity and chargeability of the semi–detailed survey (On,O,Oc,Os,Oss line)

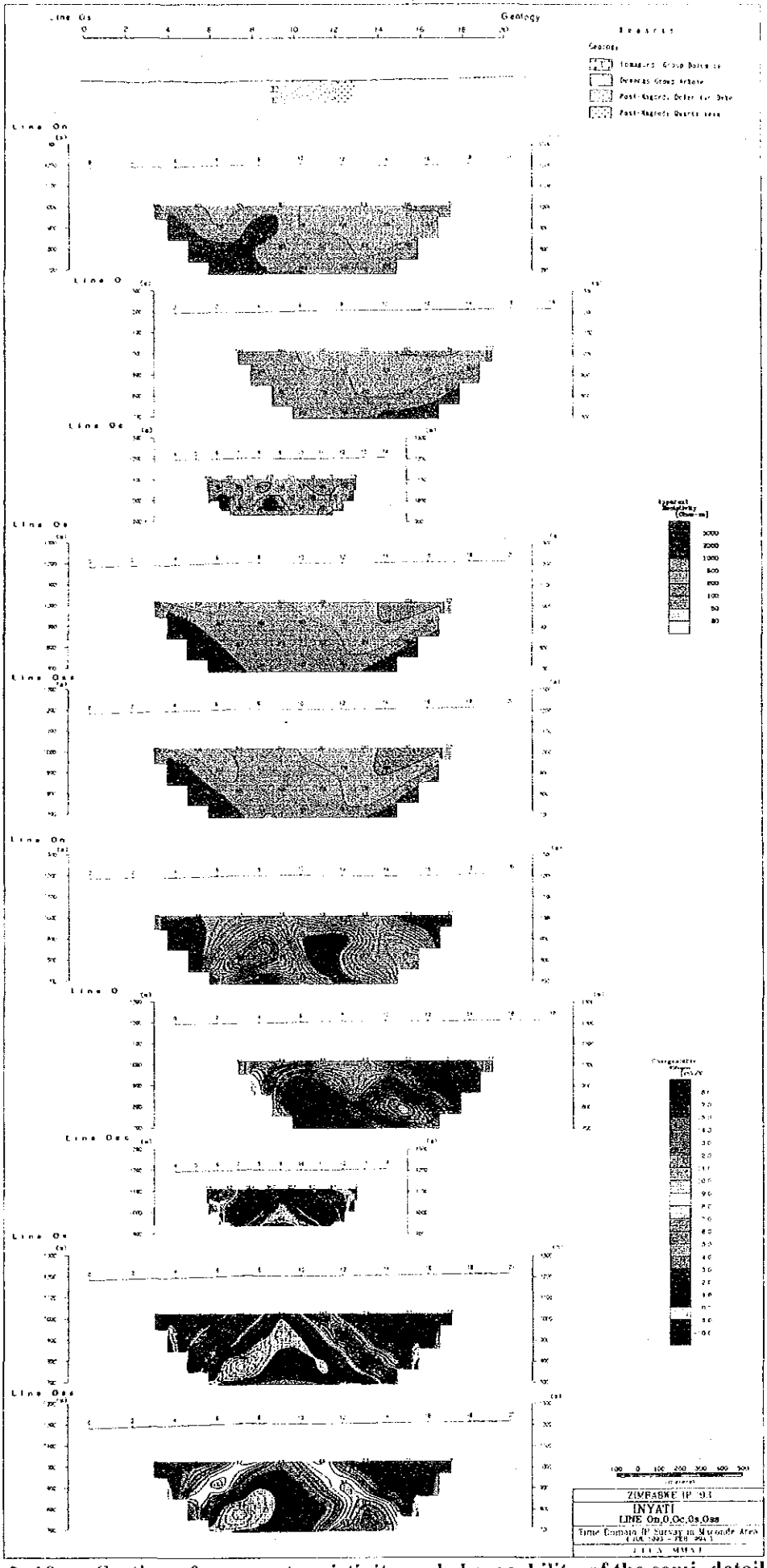

Fig.II-2-10 Section of apparent resistivity and chargeability of the semi-detailed survey (On,O,Oc,Os,Oss line)

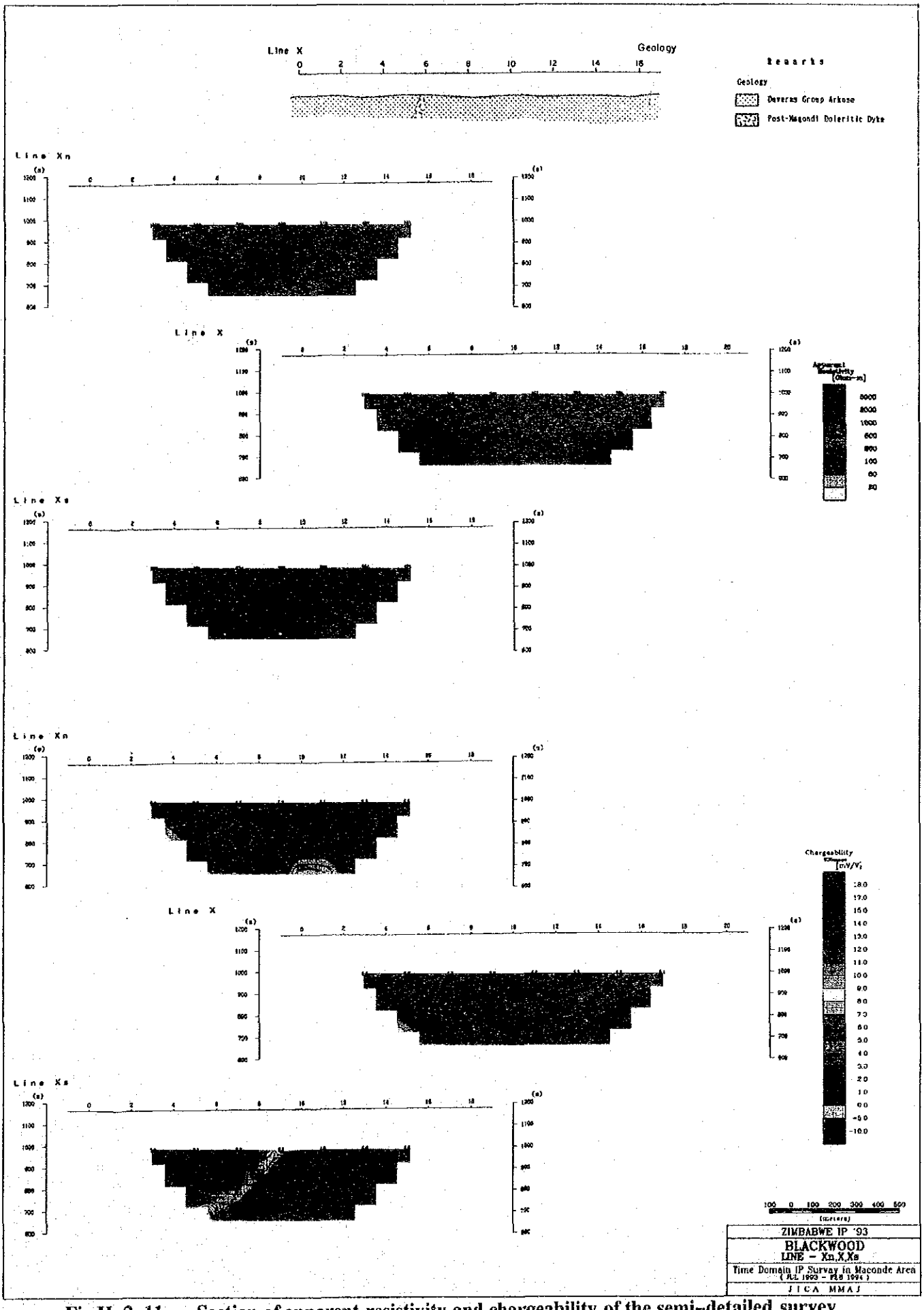

Fig.II-2-11 Section of apparent resistivity and chargeability of the semi-detailed survey (Xn,X,Xs line)

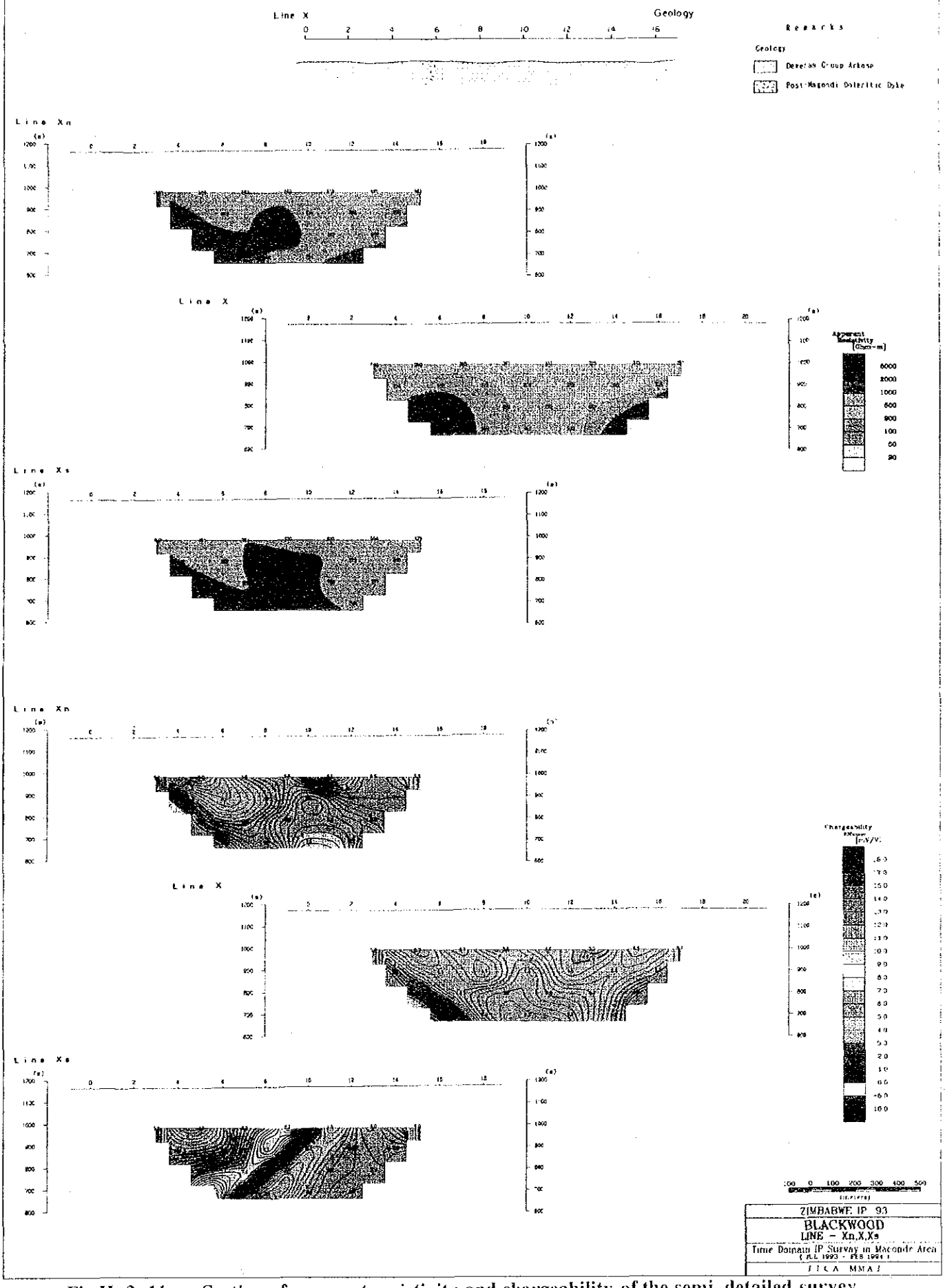

Fig.II-2-11 Section of apparent resistivity and chargeability of the semi-detailed survey (Xn,X,Xs line)

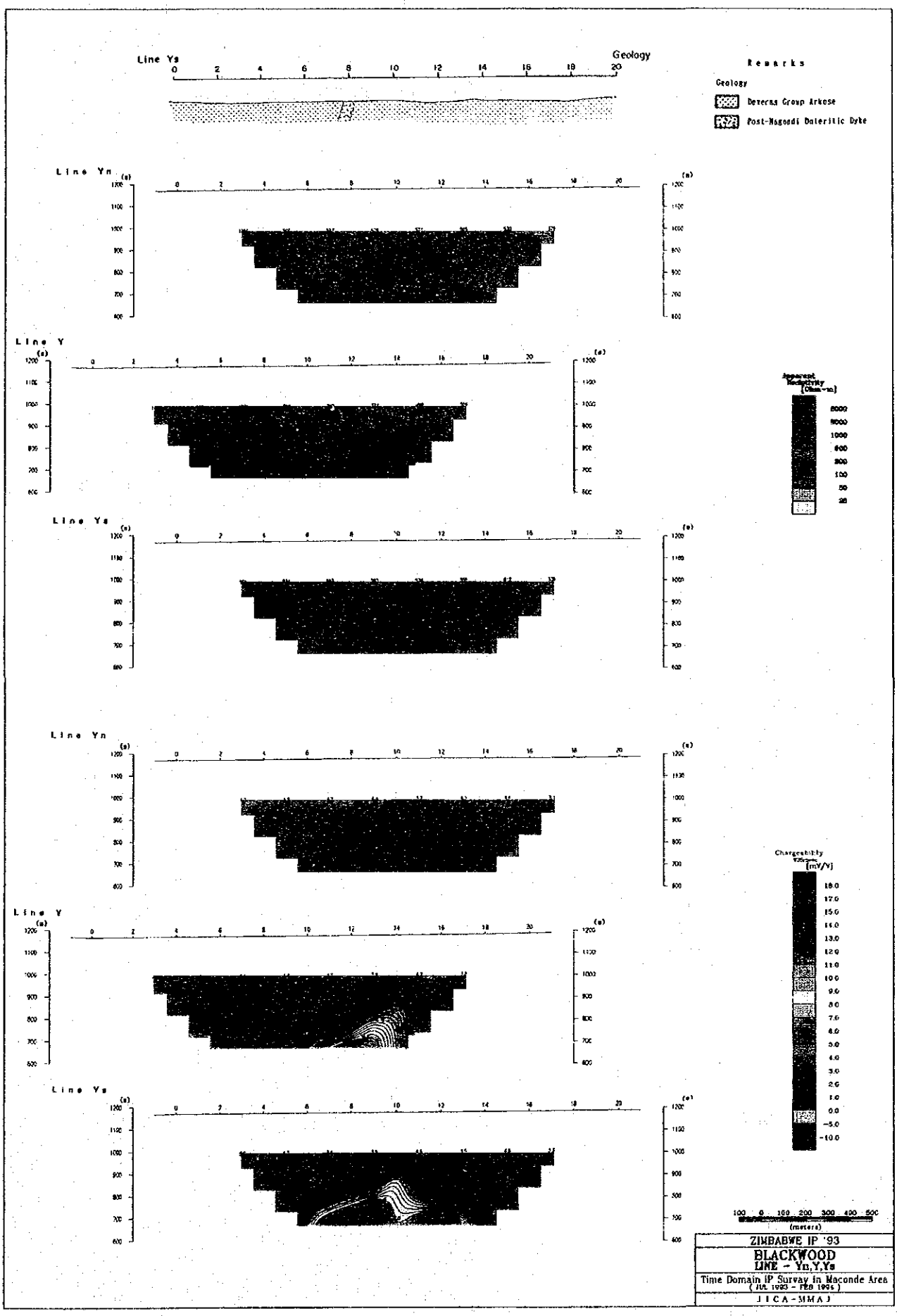

Fig.II-2-12 Section of apparent resistivity and chargeability of the semi-detailed survey (Yn,Y,Ys line)

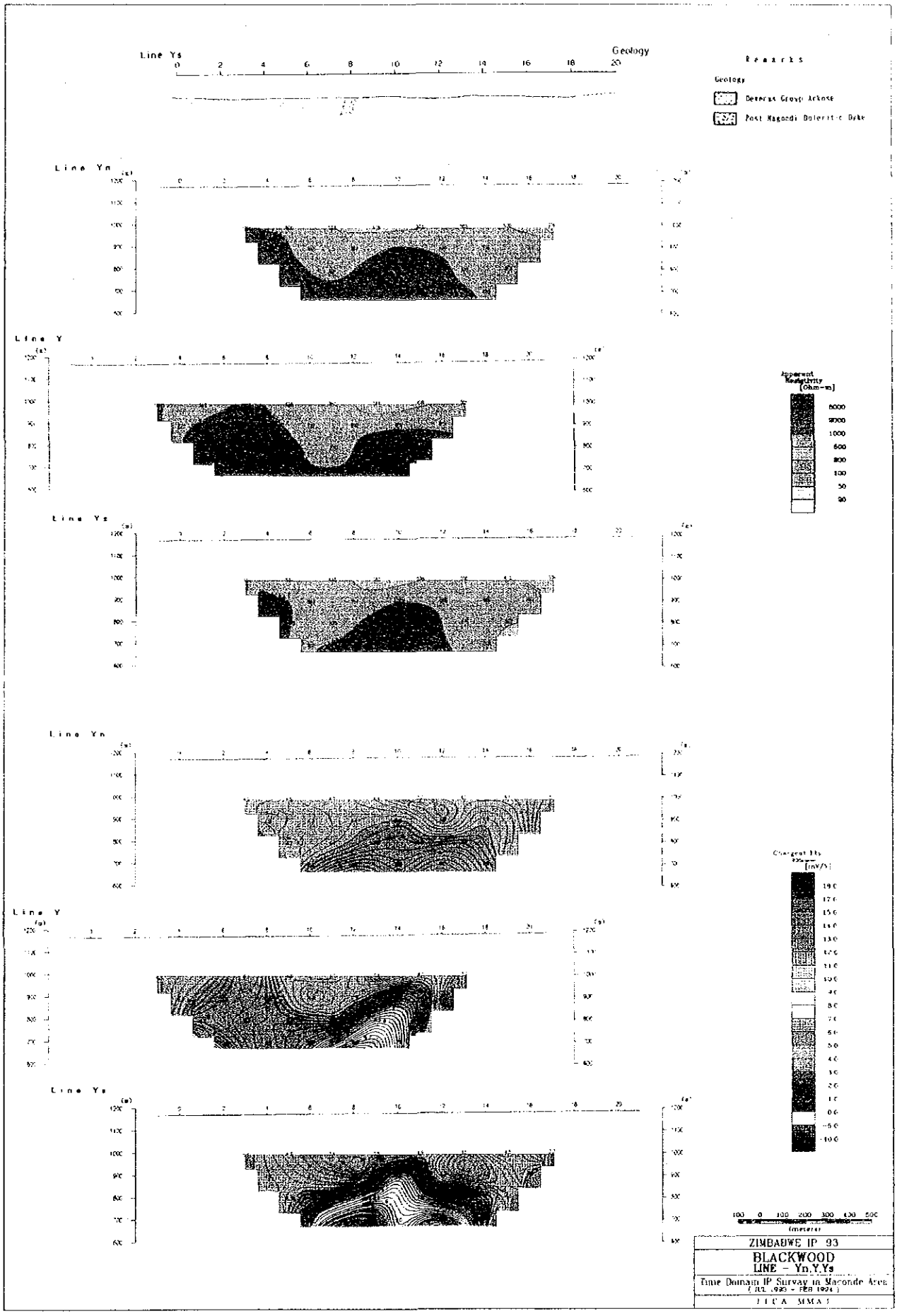

Fig.II-2-12 Section of apparent resistivity and chargeability of the semi-detailed survey (Yn.Y.Ys line)

TableII-2-5 List of the results of semi-detailed survey

Survey line	Characteristics of IP anomaly
C, Cs	No increase of IP anomaly of the deep part to the east in the station No.8 in the Cs survey line
Ln, Lc, L, Ls	Distinct pattern which wides to the deeper part of the anomaly is recognised in the station No.16 to No.19 in L(Lc) survey line. IP anomaly in each survey line suggests the continuity from the north to the south, however, the anomaly decreases in the direction of north and the south of (L,Lc)survey line.
Za	Large scale pattern which widens to the deeper part with the centre of No.0 station is recognised.
On, O, Osc, Os, Oss	Distinct pattern which widens to the deeper part of the anomaly is recognised in station No.9 of Os survey line. IP anomaly shows maximum in Os survey line and slightly decreases in the Oss survey line. Indistinct IP anomalies are recognised in O and On survey lines. Successive IP distribution with the general trend of north to south is recognised.
Xn, X, Xs	Successive distribution of IP anomalies in the direction of north to south is generally shown, however, the IP value is low.
Yn, Y, Ys	Distinct IP anomalies are recognised in the deep part. IP anomaly of the deep part is more distinct and shallower towards the south.

2. The plan of apparent resistivity and chargeability

The plan of apparent resistivity and distribution of chargeability of the sites are shown in Fig.II-2-13 to Fig.II-2-14. In the figures, the coefficient of electrodes separation selected is n=1 for the correspondence to geology.

The Binge site

Resistivity shows more than 700Ω·m respectively in the distribute area of arkose.

Resistivity shows less than 140Ω·m in the boundary of slate and sandstone of Lomagundi group in the west end of B line.

Resistivity of gneiss varies widely and does not corresponds to rock facies.

Slightly high chargeability was recognised in part of the slate of the Lomagundi group and granite of the basement.

The greenfields site

Resistivity shows more than 1,000Ω·m in the east and less than 500Ω·m in the

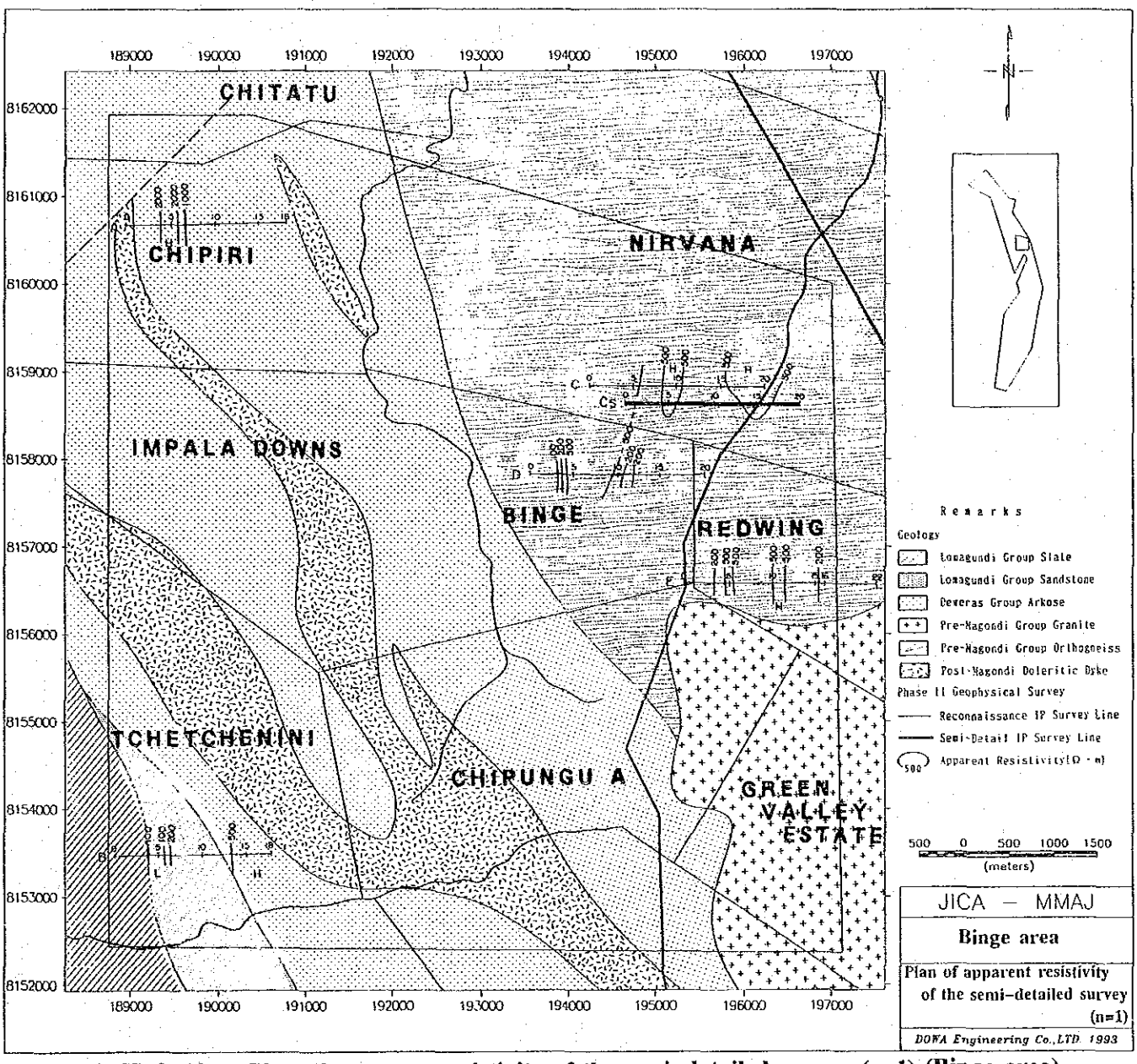

Fig.II-2-13 Plan of apparent resistivity of the semi-detailed survey (n=1) (Binge area)

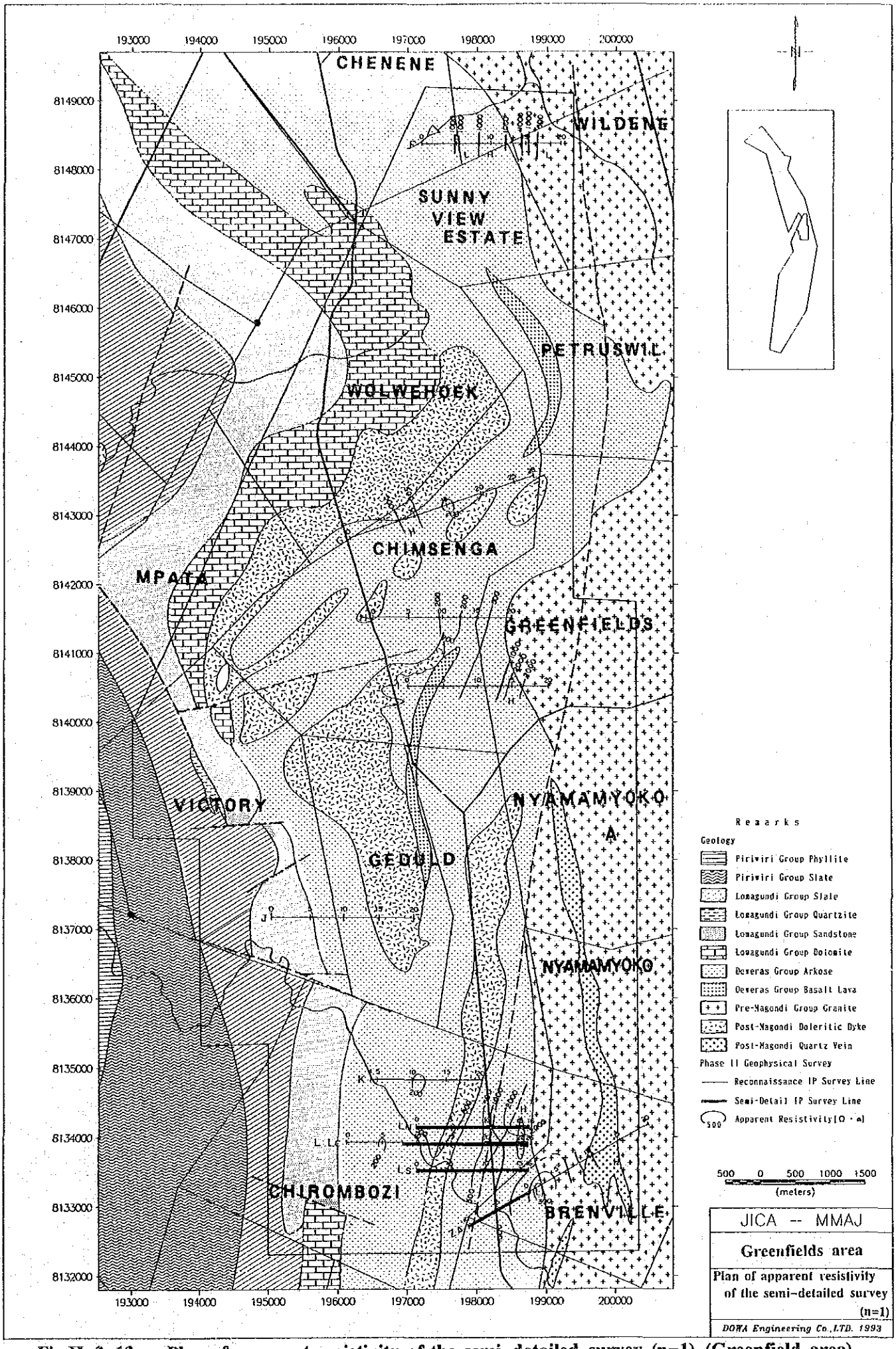

Fig.II-2-13 Plan of apparent resistivity of the semi-detailed survey (n=1) (Greenfield area)

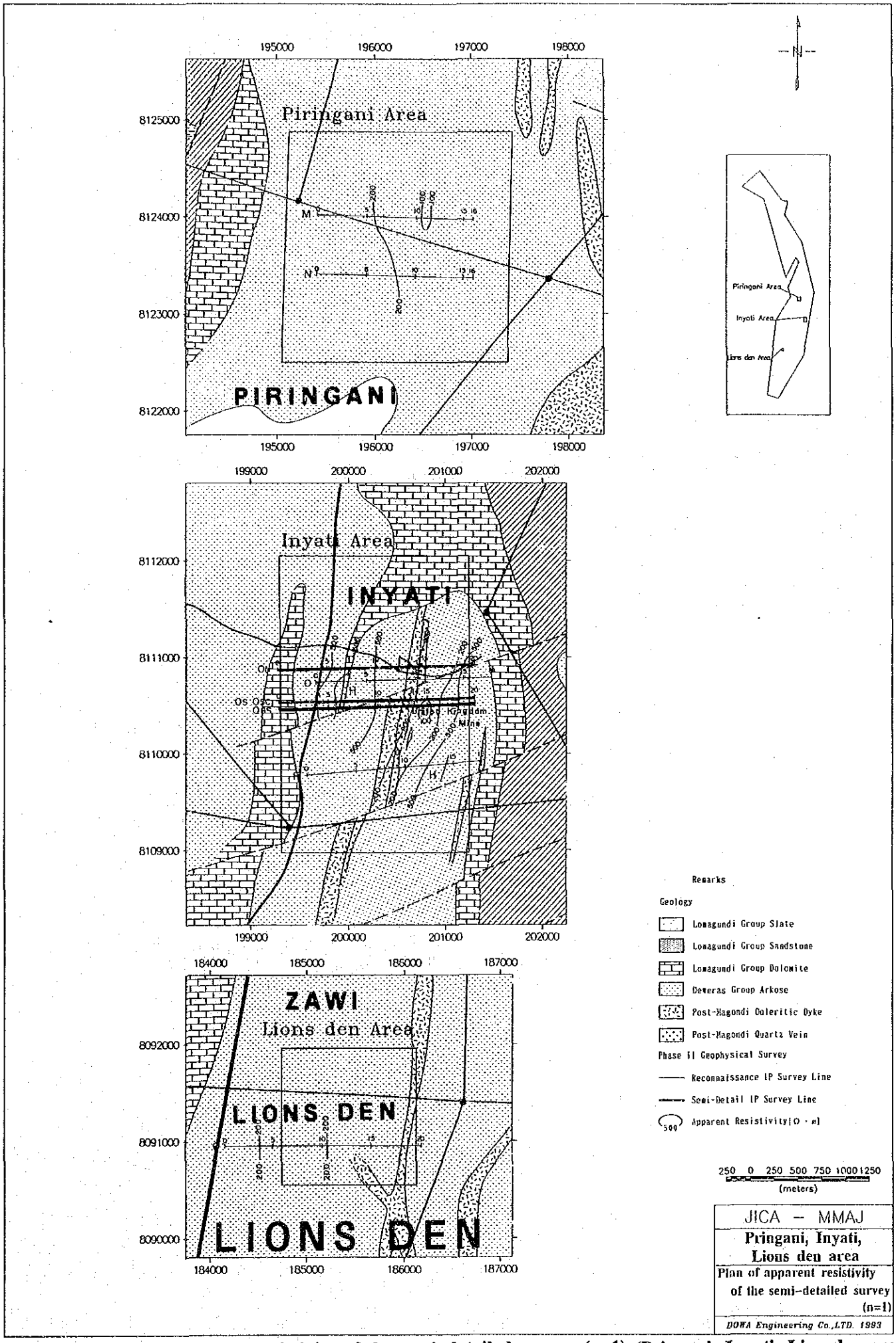

Fig.II-2-13 Plan of apparent resistivity of the semi-detailed survey (n=1) (Pringani, Inyati, Lion den area)

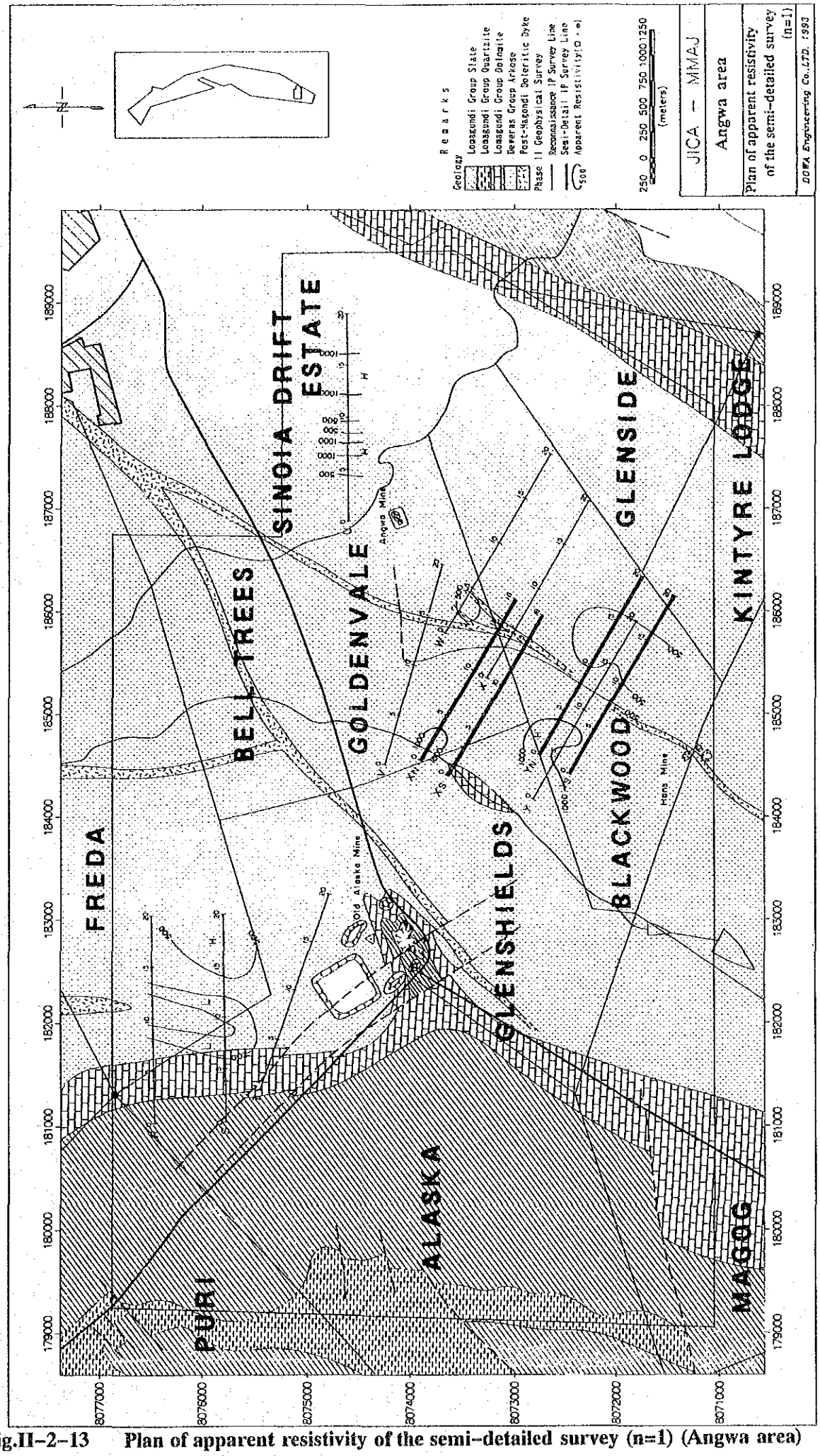

Fig.II–2–13 Plan of apparent resistivity of the semi–detailed survey (n=1) (Angwa area)

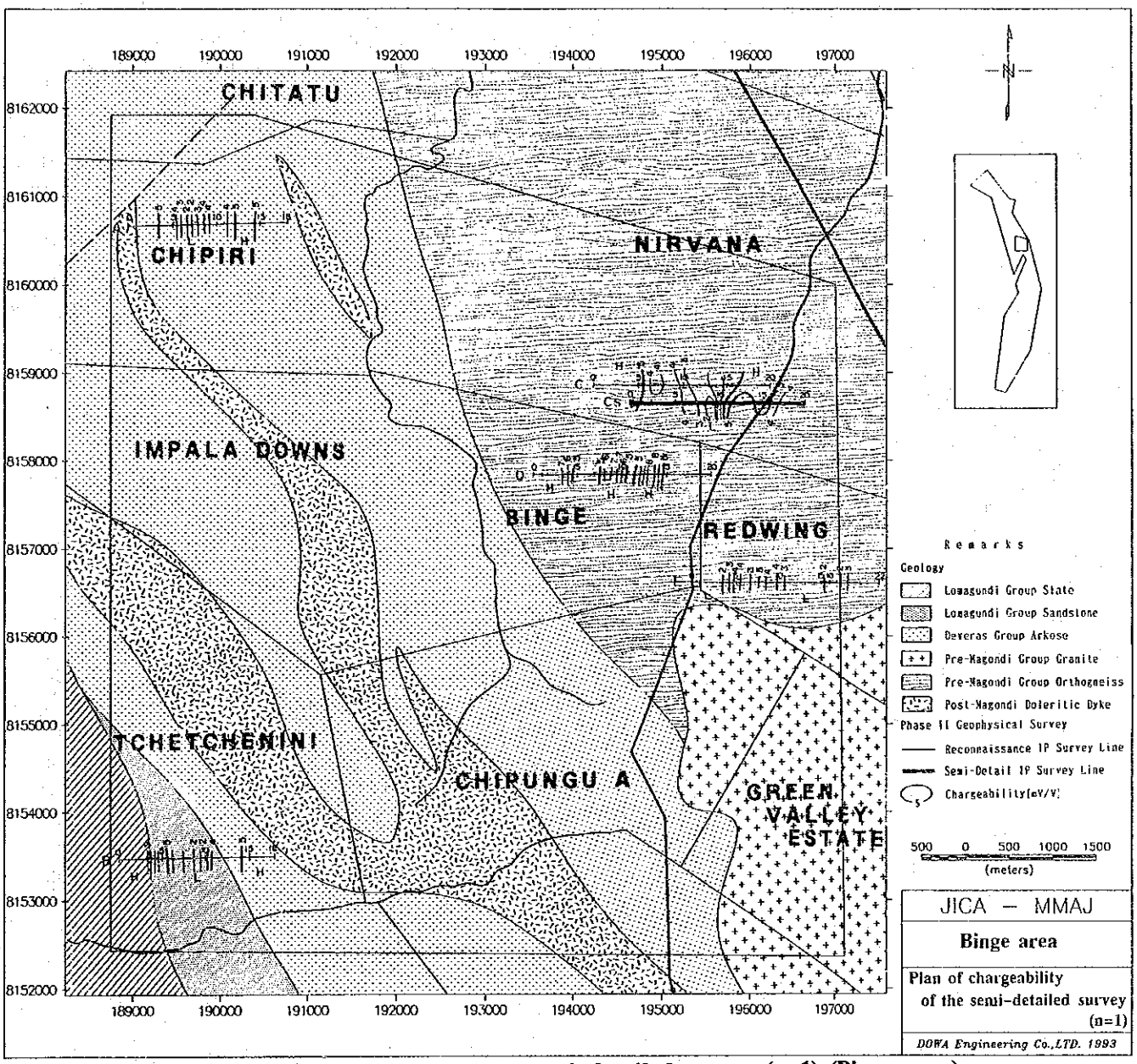

Fig.II–2–14 Plan of chargeability of the semi-detailed survey (n=1) (Binge area)

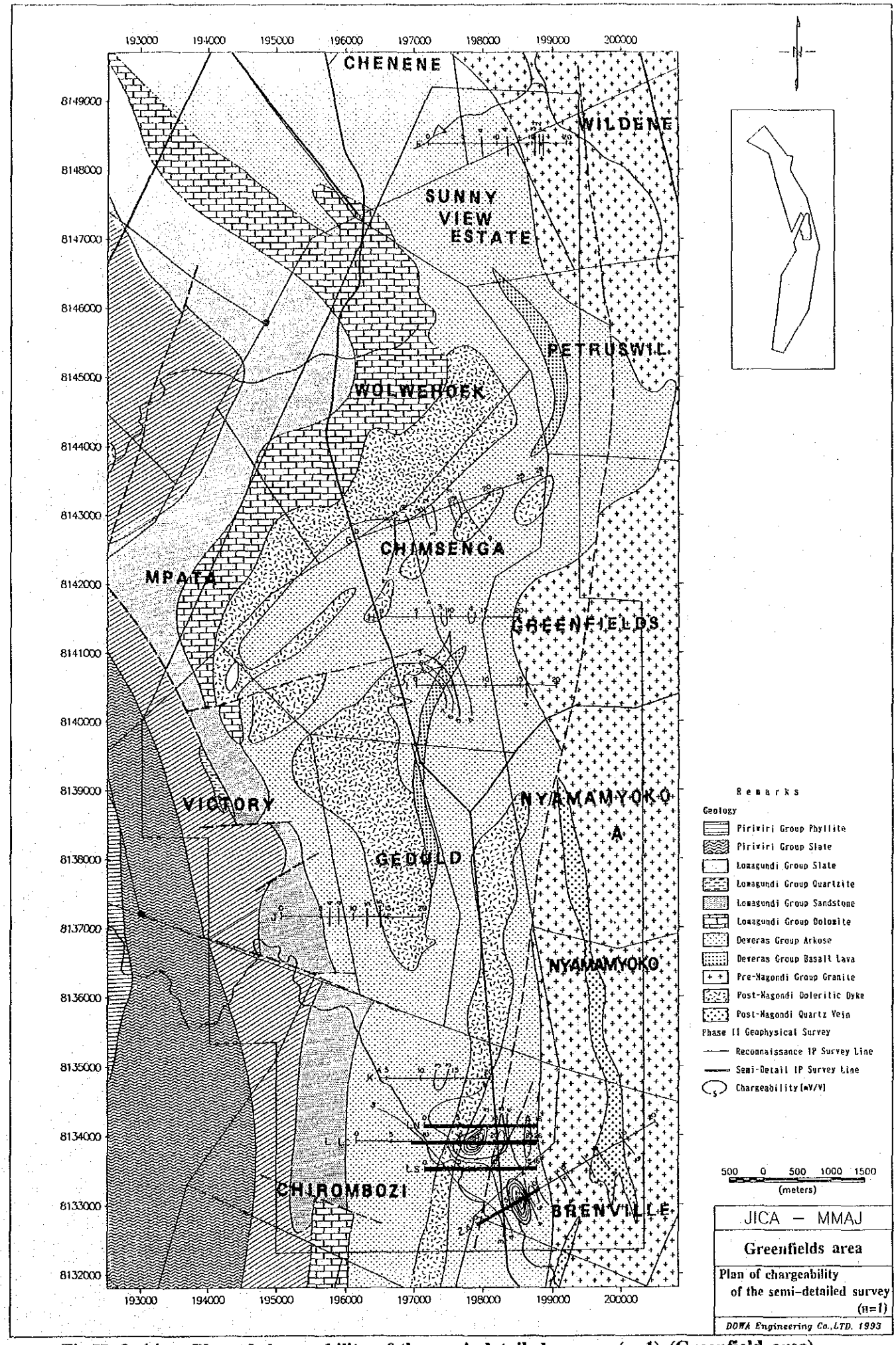

Fig.II-2-14 Plan of chargeability of the semi-detailed survey (n=1) (Greenfield area)

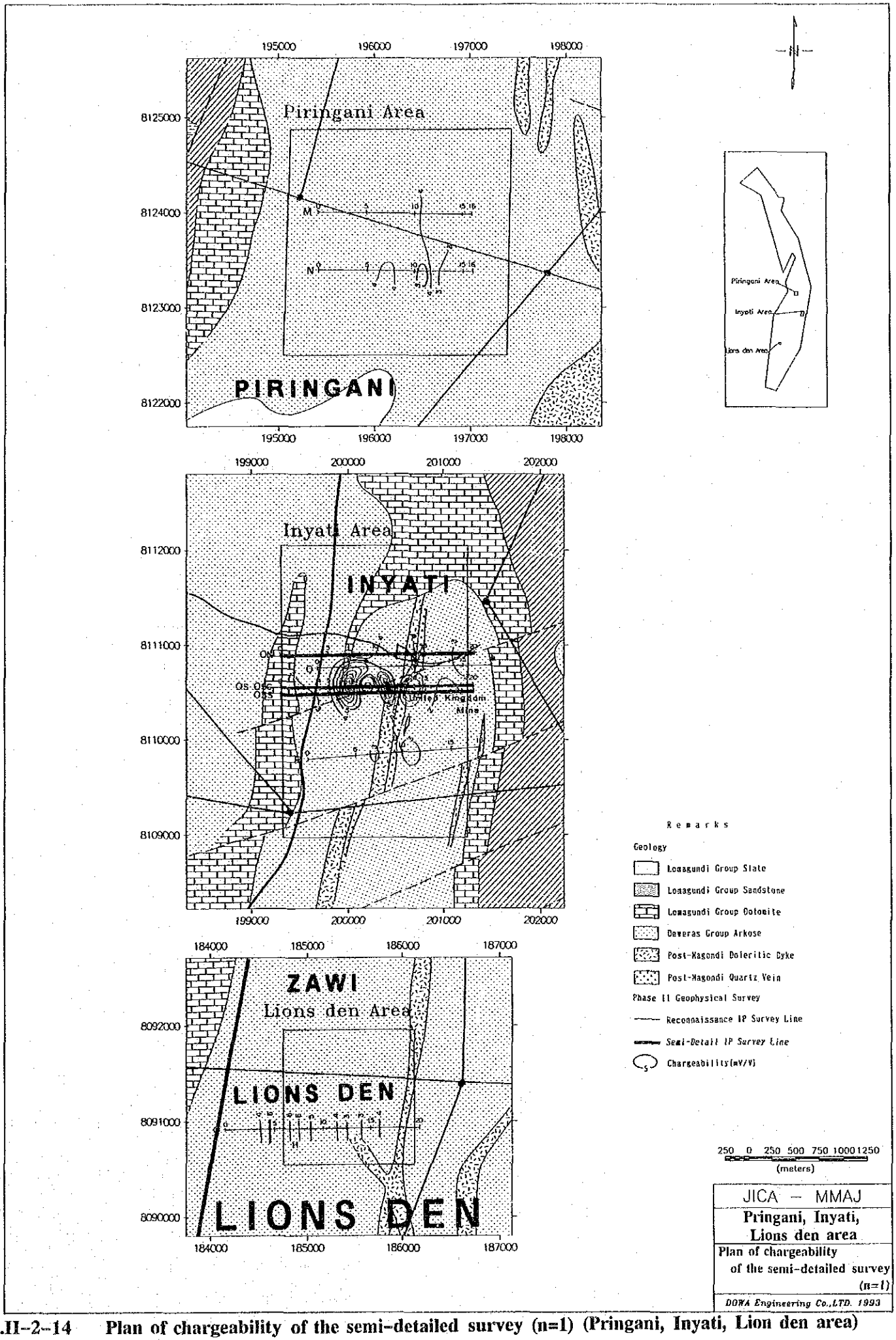

Fig.II-2-14 Plan of chargeability of the semi-detailed survey (n=1) (Pringani, Inyati, Lion den area)

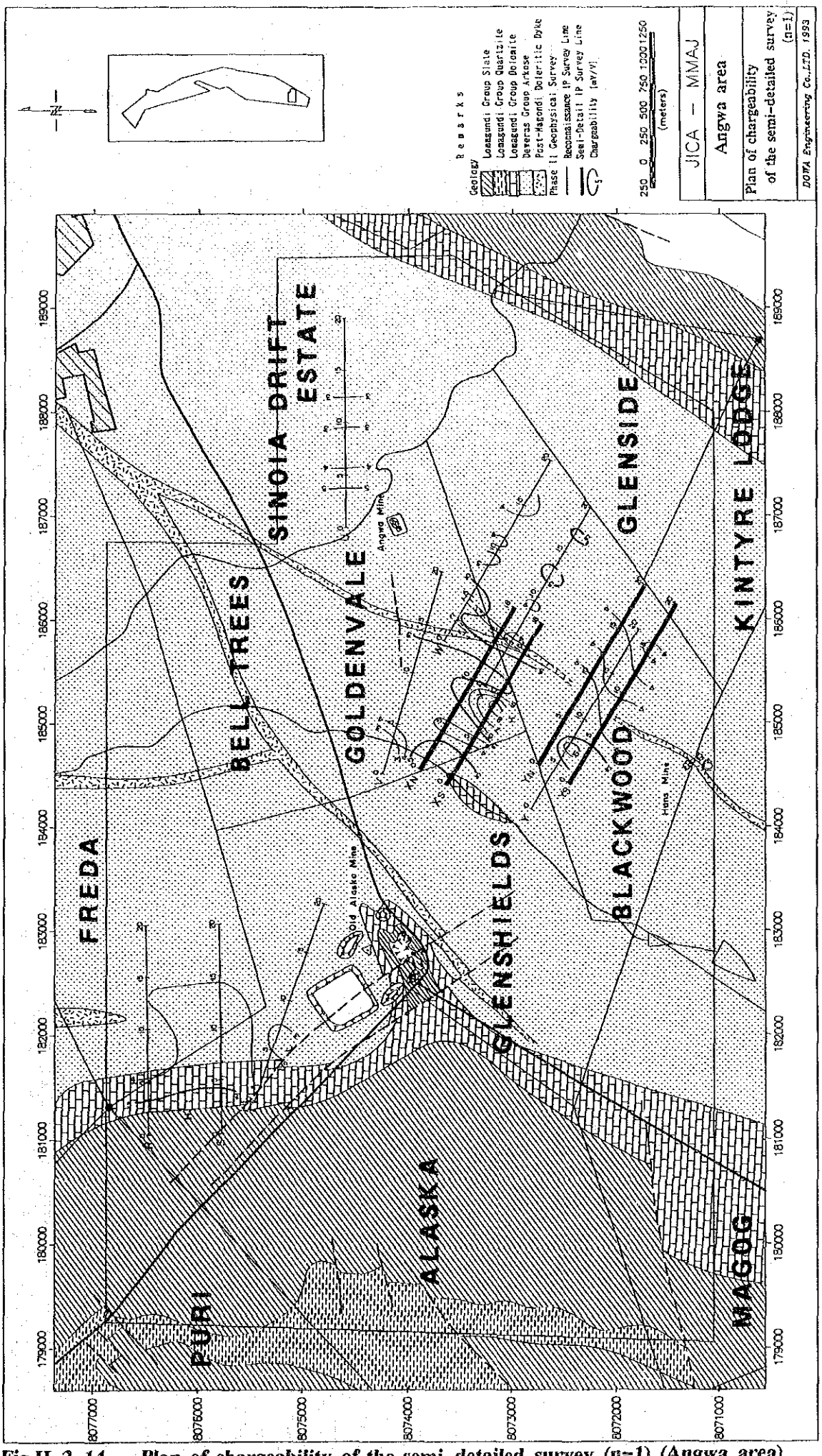

Fig.II-2-14 Plan of chargeability of the semi-detailed survey (n=1) (Angwa area)

west,respectively. The east side corresponds to the distribution area of granite of basement. The west side corresponds to the distribution area of arkose and dolerite of Deweras group.

Distinct IP anomalies were recognised in the distribution area of arkose of Deweras group.However,the succession of IP anomaly decrease to adjacent survey line.

The Primgani site

Resistivity and chargeability are constant respectively(150~300Ω·m,3~5mV/V).

The Inyati site

Arkose of Deweras group is distributed widely, dorelitic dikes and quartz vein with north to south direction are distributed in the centre part of site.

Distribution of resistivity changes to direction of east to west.

Distinct of IP anomalies, is recognised on the line Os, and Oss,and IP anomalies are very weak on the line On and P.

The Angwa site

Dolomite of Lomagundi group in the western part and arkose of the Deweras group in the eastern part of line R,S,T are distributed, respectively. However, there is no relationship between geology and the distribution of resistivity.

Slightly high chargeability(5mV/V) shows in dolomite.

Distribution of resistivity shows more than 500Ω·m in the west side and less than 500Ω·m in the east side of line V to Ys.

the distribution of resistivity changes at the dolerite dyke in distribution area of arkose.

Slightly high chargeability shows in the distribution area of the dorelite dyke.

2-2-4. Physical properties of rock and ore samples

Physical properties of rocks and ores are shown in Table II-2-6. The relationship between IP and apparent resistivity of the specimens of rocks and ore minerals is shown in Fig.II-2-15. Anisotoropy of IP and apparent resistivity is shown in Fig.II-2-16.

Resistivity of rocks varies 105 to 14,500Ω·m widely,low compacted rocks shows low resistivity and hard quartz vein and dolomite show maximum resistivity.

Chargeability of rocks shows less than 10mV/V.

Ores with oxide mineralisation show less than 5mV/V of chargeability and variety of resistivity.

Ores with sulphide mineralisation shows a tendency to low resistivity and high chargeability according to the extent of mineralisation respectively,however ores with chargeability(100mV/V) shows high resistivity more than 1,000Ω·m in the few case.

TableII-2-6 Results of physical property measurements

No.	ROCK NAME	LOCATION LAT.	LONG.	Rho (Ohm-m)	Chargeability (mV/V) m4	m5	m6	m7	m8	m9	m10	m11	m12	m13	m14
1	arkose	16 °53.31 'S	30 ° 9.59 'E	461.2	302.21	277.20	252.58	226.31	200.65	175.67	152.44	130.68	111.06	93.43	78.06
2	arkose	16 °53.31 'S	30 ° 9.59 'E	128.9	380.14	346.11	313.89	281.22	250.68	222.01	196.00	172.15	150.79	131.53	114.39
3	arkose	16 °53.31 'S	30 ° 9.59 'E	1541.6	315.47	288.71	262.51	234.56	207.16	180.20	154.93	131.17	109.86	90.91	74.71
4	arkose	16 °53.31 'S	30 ° 9.59 'E	1592.9	160.33	146.10	132.19	117.40	103.02	89.15	76.40	64.64	54.18	44.91	36.92
5	arkose	16 °53.31 'S	30 ° 9.59 'E	2520.9	102.37	89.85	78.60	67.63	57.68	48.68	40.79	33.83	27.84	22.64	18.28
6	arkose	16 °53.31 'S	30 ° 9.59 'E	809.6	53.05	43.15	34.85	27.45	21.40	16.56	12.80	9.83	7.53	5.72	4.32
7	arkose	16 °53.31 'S	30 ° 9.59 'E	2420.5	42.53	36.31	31.01	26.06	21.69	17.85	14.61	11.83	9.51	7.58	6.01
8	arkose	17 °21.56 'S	30 ° 1.33 'E	338.3	25.12	21.78	18.91	16.14	13.62	11.36	9.40	7.67	6.21	4.97	3.97
9	basalt	17 °22.43 'S	30 ° 1.57 'E	1886.3	29.36	25.06	21.53	18.16	15.22	12.64	10.43	8.52	6.92	5.57	4.46
	(anisometric measurment)			2058.7	24.60	20.43	17.06	14.03	11.48	9.37	7.64	6.26	5.11	4.19	3.44
10	conglomerate-arkose	16 °39.83 'S	30 ° 6.32 'E	1405.4	10.65	9.01	7.72	6.50	5.42	4.46	3.65	2.94	2.36	1.87	1.46
11	gneiss	16 °31.40 'S	30 ° 5.64 'E	566.2	13.98	11.86	10.14	8.50	7.05	5.78	4.69	3.76	2.99	2.34	1.82
12	gneiss	16 °30.02 'S	30 ° 7.30 'E	2435.4	19.91	17.53	15.48	13.45	11.56	9.84	8.29	6.92	5.72	4.70	3.88
	(anisometric measurment)			3037.0	15.69	13.27	11.75	10.23	8.82	7.50	6.34	5.31	4.44	3.69	3.08
13	schist,dolomitic	16 °36.56 'S	30 ° 9.87 'E	1320.2	10.22	8.60	7.32	6.10	5.03	4.09	3.29	2.61	2.04	1.58	1.22
14	quartz vein	16 °26.16 'S	30 ° 1.73 'E	14442.0	5.29	3.76	2.94	2.31	1.80	1.38	1.06	0.80	0.59	0.43	0.32
15	amphibole calc-silicate rock	16 °25.78 'S	30 ° 0.33 'E	3577.5	17.87	15.04	12.60	10.74	8.95	7.38	6.05	4.91	3.96	3.16	2.51
16	amphibole calc-silicate rock	16 °25.78 'S	30 ° 0.33 'E	105.6	618.72	574.83	528.96	477.67	425.89	374.32	325.09	278.23	234.76	195.97	153.74
	(anisometric measurment)			318.4	621.30	584.00	543.50	496.30	447.10	396.60	347.70	300.90	258.00	219.20	185.50
17	sandstone/amphibolite	16 °25.78 'S	30 ° 0.33 'E	183.3	356.99	317.30	284.19	249.37	216.03	184.49	156.07	130.42	108.11	88.80	72.72
	(anisometric measurment)			608.5	351.00	316.30	282.00	245.80	211.30	178.90	150.10	124.60	102.80	84.27	68.86
18	amphibolite	16 °25.80 'S	30 ° 1.73 'E	3930.4	54.51	46.45	39.47	32.75	26.78	21.55	17.14	13.40	10.36	7.88	5.94
	(anisometric measurment)			5371.9	50.92	43.26	36.58	30.17	24.51	19.55	15.41	11.95	9.17	6.93	5.18
19	dolomite	17 °23.87 'S	30 ° 0.87 'E	2852.5	13.38	11.24	9.54	7.94	6.53	5.31	4.28	3.40	2.70	2.09	1.63
20	arkose with malachite	16 °52.31 'S	30 ° 9.59 'E	2463.5	8.04	6.63	5.56	4.60	3.76	3.02	2.44	1.93	1.51	1.17	0.90
21	quartzite	16 °58.27 'S	30 °12.62 'E	3168.8	3.86	3.12	2.63	2.16	1.78	1.42	1.13	0.89	0.67	0.51	0.37
22	arkose-slate	16 °52.43 'S	30 ° 9.80 'E	835.3	22.57	19.33	16.57	13.90	11.51	9.41	7.61	6.07	4.79	3.73	2.88
23	granodiorite	16 °53.61 'S	30 °10.20 'E	3632.3	15.16	13.16	11.31	9.74	8.28	6.95	5.81	4.79	3.90	3.22	2.60
24	arkose	16 °55.03 'S	30 ° 9.12 'E	1724.6	19.04	15.82	13.26	10.95	8.98	7.31	5.91	4.74	3.77	2.98	2.32
25	slate,graphitic	16 °56.44 'S	30 ° 6.15 'E	1243.7	55.75	51.38	40.10	30.66	23.22	17.48	13.10	9.78	7.28	5.41	4.01
	(anisometric measurment)			1745.9	150.00	121.40	97.02	75.13	57.11	42.74	31.62	23.12	16.76	12.01	8.55
26	amhibolitic rock	16 °56.21 'S	30 ° 9.16 'E	1845.9	120.43	108.31	97.05	85.58	74.76	64.60	55.41	47.02	39.60	33.04	27.41
	(anisometric measurment)			739.7	598.70	561.70	521.60	474.90	426.40	376.60	328.50	282.40	240.30	201.80	168.30
27	arkose	16 °56.21 'S	30 ° 9.16 'E	2432.8	66.14	56.40	48.19	40.59	33.98	28.23	23.34	19.14	15.60	12.61	10.29
	(anisometric measurment)			2797.6	39.40	32.30	26.52	21.37	17.07	13.52	10.67	8.38	6.55	5.11	3.99
28	quartz vein in doleritic rock	16 °56.21 'S	30 ° 9.16 'E	6954.6	25.14	21.64	18.73	15.93	13.41	11.15	9.21	7.53	6.12	4.95	3.91
	(anisometric measurment)			380.9	528.00	489.70	450.30	406.30	361.90	317.00	274.30	233.50	196.30	162.80	133.50
29	arkose	16 °56.21 'S	30 ° 9.16 'E	3505.3	33.59	29.32	25.71	22.24	19.08	16.19	13.64	11.35	9.36	7.63	6.19
30	arkose	16 °56.21 'S	30 ° 9.16 'E	308.3	759.50	728.94	694.22	651.47	604.51	553.10	500.58	446.67	394.27	343.51	297.49
	(anisometric measurment)			339.5	855.10	827.90	795.90	755.09	708.50	656.10	601.10	543.40	486.10	429.20	375.30
31	doleritic basalt with sulphides	16 °57.21 'S	30 ° 9.52 'E	1392.0	153.87	135.61	119.51	104.21	90.61	78.46	67.82	58.28	49.88	42.42	36.04
	(anisometric measurment)			2572.8	96.58	84.45	73.65	63.17	53.75	45.33	38.06	31.68	26.27	21.66	17.80
32	arkose	16 °53.31 'S	30 ° 9.59 'E	3641.6	20.05	16.97	14.48	12.17	10.14	8.36	6.84	5.54	4.45	3.54	2.81
33	arkosearkose	16 °53.31 'S	30 ° 9.59 'E	5642.0	26.28	22.65	19.57	16.60	13.91	11.50	9.42	7.63	6.12	4.86	3.89
34	arkose-conglomerate	16 °53.31 'S	30 ° 9.59 'E	12800.2	104.65	92.99	82.48	71.99	62.26	53.27	45.26	38.06	31.78	26.28	21.83
	(aniscaetric measurment)			16963.4	110.60	98.28	86.99	75.73	65.29	55.68	47.15	39.53	32.92	27.18	22.33
35	arkose	16 °53.31 'S	30 ° 9.59 'E	2784.8	28.89	23.72	19.47	15.65	12.42	9.78	7.62	5.90	4.54	3.46	2.62
36	arkose	17 °22.47 'S	30 ° 1.59 'E	569.5	7.46	6.04	4.99	4.08	3.32	2.69	2.16	1.73	1.37	1.07	0.84
37	arkose(malachitization)	17 °22.47 'S	30 ° 1.95 'E	583.3	7.98	6.58	5.53	4.59	3.77	3.08	2.50	2.01	1.61	1.27	1.03
38	arkose(malachitization)	17 °22.47 'S	30 ° 1.95 'E	777.0	6.96	5.80	4.92	4.10	3.39	2.76	2.23	1.78	1.41	1.10	0.86
39	arkose(malachitization)	17 °22.47 'S	30 ° 1.95 'E	1247.6	4.59	3.75	3.17	2.62	2.14	1.71	1.37	1.07	0.81	0.60	0.35
40	arkose	17 °32.96 'S	30 ° 3.37 'E	7665.3	27.93	23.91	20.61	17.47	14.69	12.22	10.11	8.27	6.74	5.45	4.43
	(anisometric measurment)			6672.9	22.67	19.06	16.11	13.38	10.97	8.94	7.25	5.85	4.72	3.80	3.04
41	arkose	17 °32.96 'S	30 ° 3.37 'E	4938.0	246.00	219.86	194.89	169.30	145.34	123.18	103.57	86.16	71.20	58.36	47.96
	(anisometric measurment)			6613.7	246.10	222.20	199.10	174.90	151.80	129.80	110.00	92.00	76.30	62.64	51.08
42	qurtz vein in doleritic rock	17 °32.96 'S	30 ° 3.37 'E	5426.9	128.40	115.50	103.45	91.19	79.75	69.17	59.78	51.38	44.05	37.59	32.19
	(anisometric measurment)			4260.0	101.60	89.82	79.38	69.28	60.13	51.82	44.51	37.98	32.29	27.32	23.08
43	qurtz-bornite vein in arkose	17 °32.96 'S	30 ° 3.37 'E	6236.5	72.31	62.40	53.84	45.74	38.55	32.20	26.74	22.01	17.99	14.59	11.95
	(anisometric measurment)			17329.0	76.35	65.90	56.83	48.19	40.54	33.81	28.06	23.11	18.93	15.40	12.47
44	quartz vein	17 ° 4.67 'S	30 °11.24 'E	14500.5	10.33	8.64	7.52	6.47	5.53	4.68	3.92	3.26	2.69	2.21	1.88
45	dolomite(malachitization)	17 °23.87 'S	30 ° 0.87 'E	1988.8	19.21	16.20	13.70	11.37	9.32	7.57	6.09	4.85	3.83	2.99	2.33
46	dolomite(malachitization)	17 °23.87 'S	30 ° 0.87 'E	480.7	20.29	16.96	14.19	11.60	9.35	7.51	5.96	4.66	3.63	2.78	2.14
47	dolomite(malachitization)	17 °23.87 'S	30 ° 0.87 'E	1523.5	24.77	20.68	17.29	14.17	11.49	9.19	7.30	5.73	4.45	3.42	2.60
48	dolomite(malachitization)	17 °23.87 'S	30 ° 0.87 'E	3126.8	18.96	15.87	13.40	11.13	9.13	7.41	5.97	4.75	3.75	2.93	2.30
49	arkose with quartz vein	17 °17.86 'S	30 ° 4.11 'E	2157.6	23.14	19.71	16.86	14.18	11.80	9.72	7.95	6.41	5.12	4.07	3.21
50	arkose	17 °17.86 'S	30 ° 4.11 'E	5476.1	55.83	48.81	42.65	36.64	31.17	26.23	21.92	18.13	14.89	12.12	9.90
	(anisometric measurment)			6573.1	45.71	39.43	34.04	28.87	24.27	20.19	16.69	13.69	11.17	9.06	7.31
51	sandstone	17 °21.75 'S	30 ° 6.88 'E	5848.2	35.80	31.35	27.52	23.80	20.41	17.33	14.62	12.21	10.15	8.36	6.88
	(anisometric measurment)			5481.9	29.20	24.95	21.41	18.08	15.13	12.57	10.38	8.53	6.97	5.66	4.60
52	dolomite	17 °19.85 'S	30 ° 8.85 'E	11269.9	22.40	19.59	17.30	15.03	12.92	10.97	9.23	7.67	6.32	5.16	4.28
	(anisometric measurment)			16754.2	12.64	10.48	8.93	7.51	6.24	5.13	4.21	3.43	2.78	2.25	1.82
53	qurtzite	17 °20.43 'S	30 ° 9.04 'E	8853.4	21.91	18.92	16.45	14.05	11.87	9.90	8.18	6.68	5.40	4.31	3.47
54	qurtzite	17 °13.05 'S	30 ° 8.70 'E	3259.5	14.69	12.55	10.80	9.16	7.66	6.38	5.23	4.27	3.45	2.75	2.16
55	dolerite	16 °56.75 'S	30 °11.63 'E	1120.5	41.31	35.01	29.71	24.79	20.44	16.70	13.59	10.92	8.73	6.93	5.47
	(anisometric measurment)			1563.7	36.93	30.75	25.65	20.97	16.96	13.56	10.77	8.49	6.68	5.22	4.12
56	granodiorite	16 °48.31 'S	30 °10.99 'E	5686.8	6.10	5.00	4.24	3.56	2.95	2.42	1.96	1.56	1.20	0.96	0.76
57	slata	17 °16.56 'S	30 ° 0.20 'E	128.3	40.20	32.49	26.49	21.30	17.02	13.60	10.81	8.55	6.72	5.23	4.08
58	dolomite	17 °19.23 'S	30 ° 6.28 'E	11736.3	2.13	1.10	0.77	0.56	0.39	0.25	0.16	0.08	0.02	-0.02	-0.03
59	sandy slate origin mica schist	16 °56.42 'S	30 ° 5.71 'E	375.9	28.49	23.82	19.84	16.16	13.00	10.34	8.16	6.37	4.93	3.78	2.88
60	basalt with elongated amygdal	17 °30.91 'S	29 °57.42 'E	1061.5	21.46	18.43	15.88	13.44	11.26	9.33	7.66	6.22	5.00	3.98	3.16
	(anisometric measurment)			2278.1	12.43	9.84	7.86	6.15	4.73	3.59	2.73	2.07	1.57	1.16	0.85

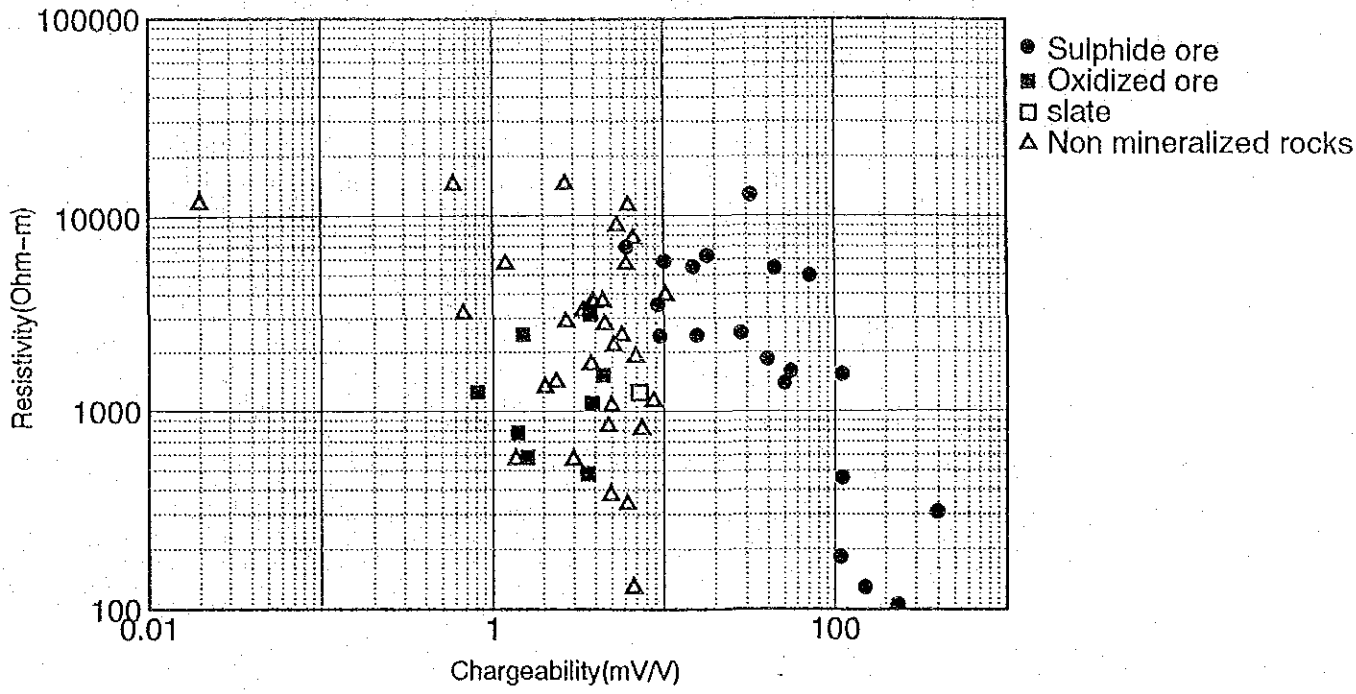

Fig.II-2-15 Relationship between IP and apparent resistivity of rock and ore samples

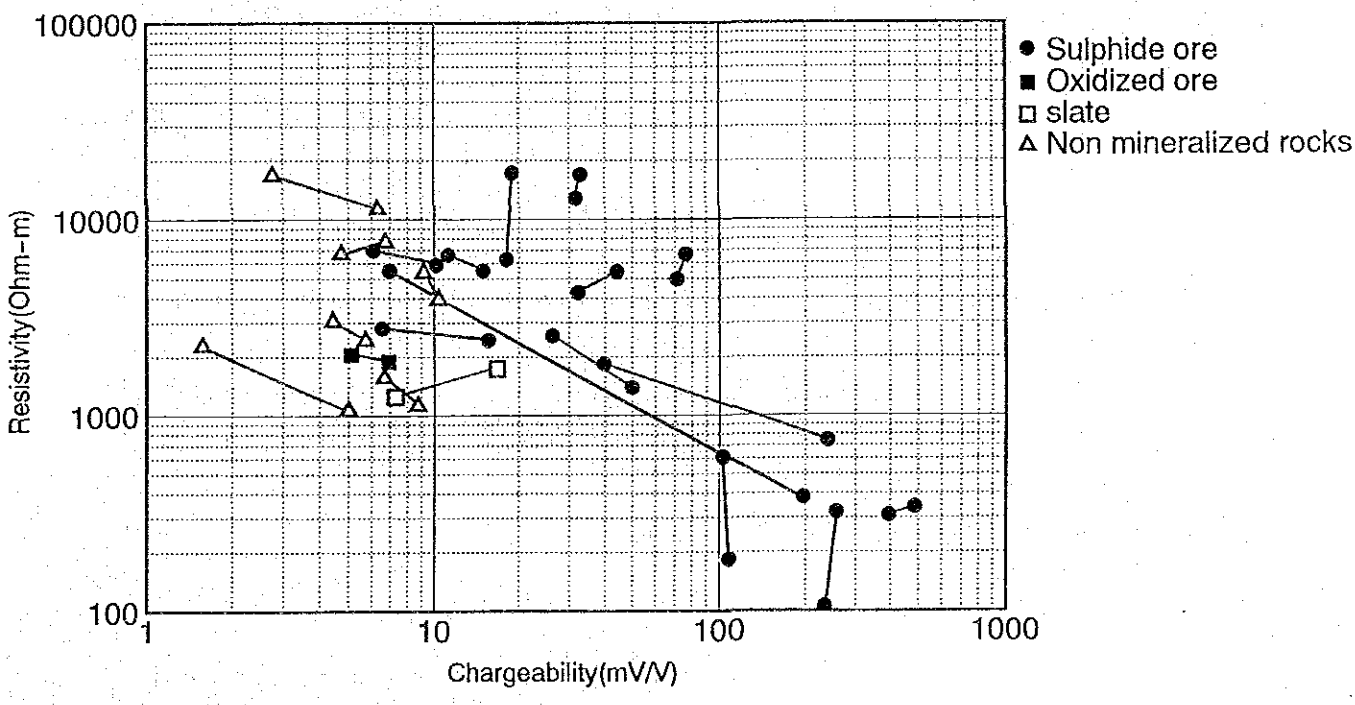

Fig.II-2-16 Anisotropy of IP and apparent resistivity of rock and ore samples

In some case,samples shows variety of physical property by the direction of transmit a electricity,in the case of same direction of transmition and mineralisation,Ore samples shows a tendency to distinct low resistivity high chargeability.Ore of quartz vein has maximum variety,and shows 300 to 7,000Ω·m of resistivity and 5 to 200mV/V of chargeability.Rock samples of graphite slate shows about same chargeability(16.8mV/V) to the weak mineralised ore samples,bay the direction of transmition of electricity.

2-2-5. Results of data processing

1. 2.5 Dimensional section analysis of apparent resistivity/IP anomaly

Sectional analysis of simulation model was carried out by 2.5 dimensional finite element method for apparent resistivity/chargeability of provisional sections of 6 survey lines of B, C, L, O, Za and Ys which were selected within IP anomalous zones by reconnaissance and semi-detailed prospecting. Physical properties of rocks and ore samples are used for this analyses as a reference.

The result is shown in Fig.II-2-17.

(1) B survey line(Fig.II-2-17(2))

There are two layers of resistivity. The surface layer shows low resistivity(less than 300 Ω·m). The lower layer has high resistivity
(more than 3,000Ω·m).

The IP anomalous pattern of the deep part in the station No.8 generally matched by the assumption of existence of IP anomalous body(10mV/V) in the stations No.0 to No.2 and low IP body in the stations No.8 to No.10.

The area from the stations No.0 to No.10 corresponds to graphitic slate of the Lomagundi group.

(2) C survey line(Fig.II-2-17(2))

There are three layers of resistivity. The surface two layers show low resistivity less than 180 Ω·m and 750 Ω·m. The resistivity of the lower layer is 4,000Ω·m.

The IP anomalous pattern of the deep part in the station No.12 to No.14 generally matched by the assumption of existence of low IP anomalous body in the surface area and anomalous body of 20mV/V in the lower layer.

The Pre-Magondi gneiss is distributed in this area.

(3) L survey line(Fig.II-2-17(3))

The structure of resistivity in this site is presumed that one block less than 500Ω·m is on the surface and the western deep part of the station No.19. The other block with resistivity of 4,000 Ω·m is presumed to be in the eastern deep part of the station No.19.

The IP anomalous pattern in the station No.18 to No.19 generally matched by the assumption of existence of low IP anomalous body of 70mV/V on a small scale near the surface and fairly high anomalous body in surrounded area.

(4) Za survey line(Fig.II-2-17(4))

The resistivity suggests that the structure is composed of two blocks. One block is near the IP anomalous part with 500Ω·m and the other is 3,000Ω·m part.

The IP anomalous pattern corresponds to the assumption of the existence of a flat anomalous body(300mV/V) with fair inclination at a depth of 200m. The scale of the anomalous body is comparatively large.

The geology comprise the basement granite in the eastern part and arkose in the western part.

IP anomaly corresponds to the boundary area of arkose and granite.

(5) Os survey line(Fig.II-2-17(5))

There are two layer of resistivity. The resistivity of the surface layer is 5000 Ω·m and that of the lower layer is 4,000 Ω·m.

The IP anomalous patterns generally matched the assumption of the existence of anomalous body of 150mV/V with steep inclination in the stations No.8 to No.10.

The geology comprise arkose, doleritic dykes and quartz-calcite veins of the Deweras group with basic intrusive rocks in the central part of the survey line. Quartz-calcite veins were recognised on the surface nearby the IP anomaly.

(6) Ys survey line(Fig.II-2-17(6))

The matching was necessary to presume a complex structure of resistivity and chargeability. Fundamental resistivity is composed of three blocks with 130 to 280Ω·m, 750Ω·m and 2,500 Ω·m, respectively.

The IP anomalous body is presumed to be a flat body with steep inclination more than 200m in depth.

2-3. Consideration

Distinct IP anomalous zones was detected by extension of the existing survey lines and the setting up of new survey lines adjacent to the existing survey lines which are presumed to have detected the whole or a part of the IP anomalies.

Distinct IP anomalous patterns were shown in the Binge site (B, C, Cs survey lines), the Greenfields site(L, Za survey lines), the Inyati site(O, Os, Oss survey lines) and the Angwa site(Y,Ys survey lines). In addition to the lines, comparatively distinct IP anomalous zones were detected in Xn, X and Xs lines of the Angwa site.

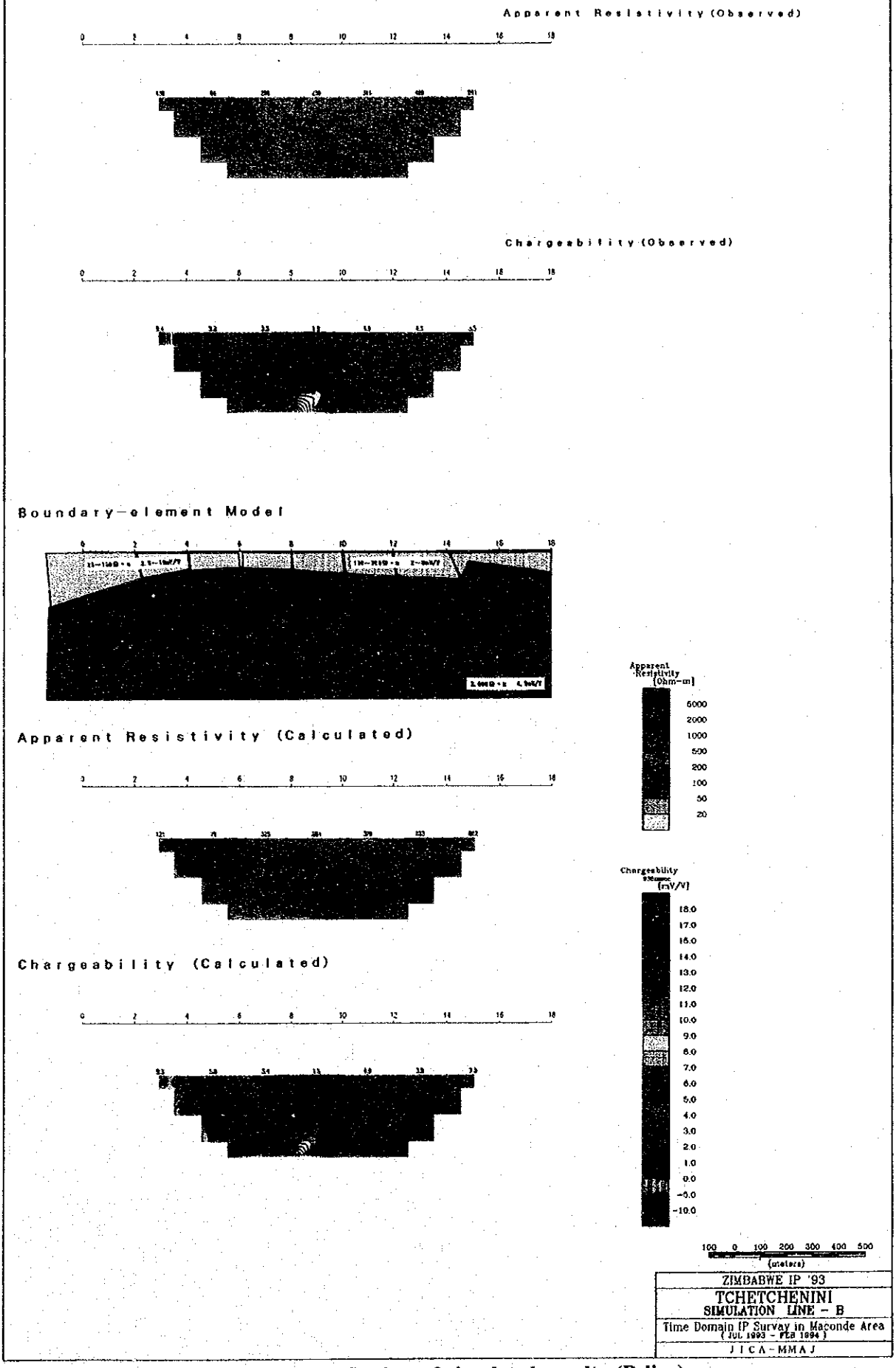

Fig.II-2-17 Section of simulated results (B line)

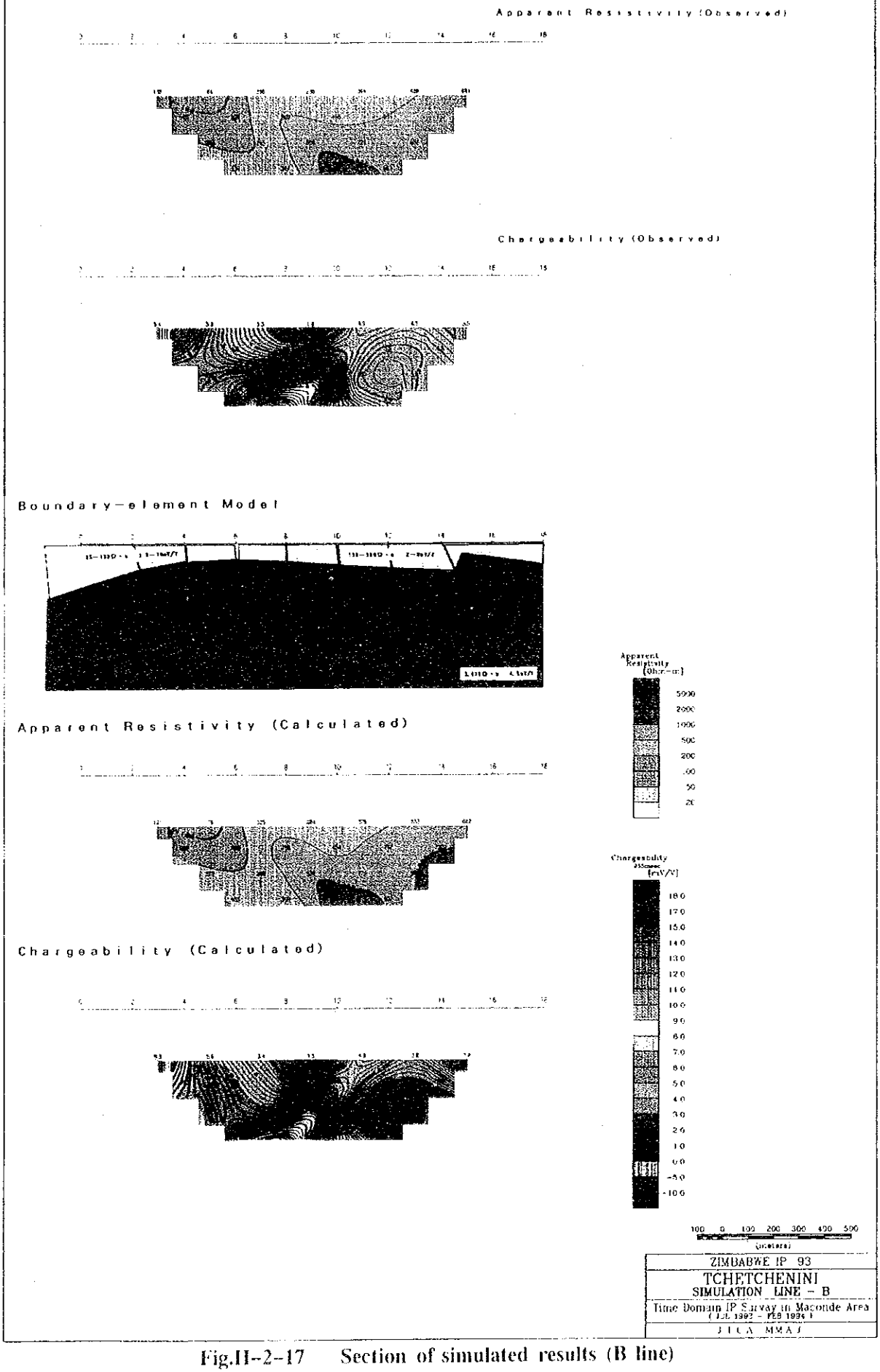

Fig.II-2-17 Section of simulated results (B line)

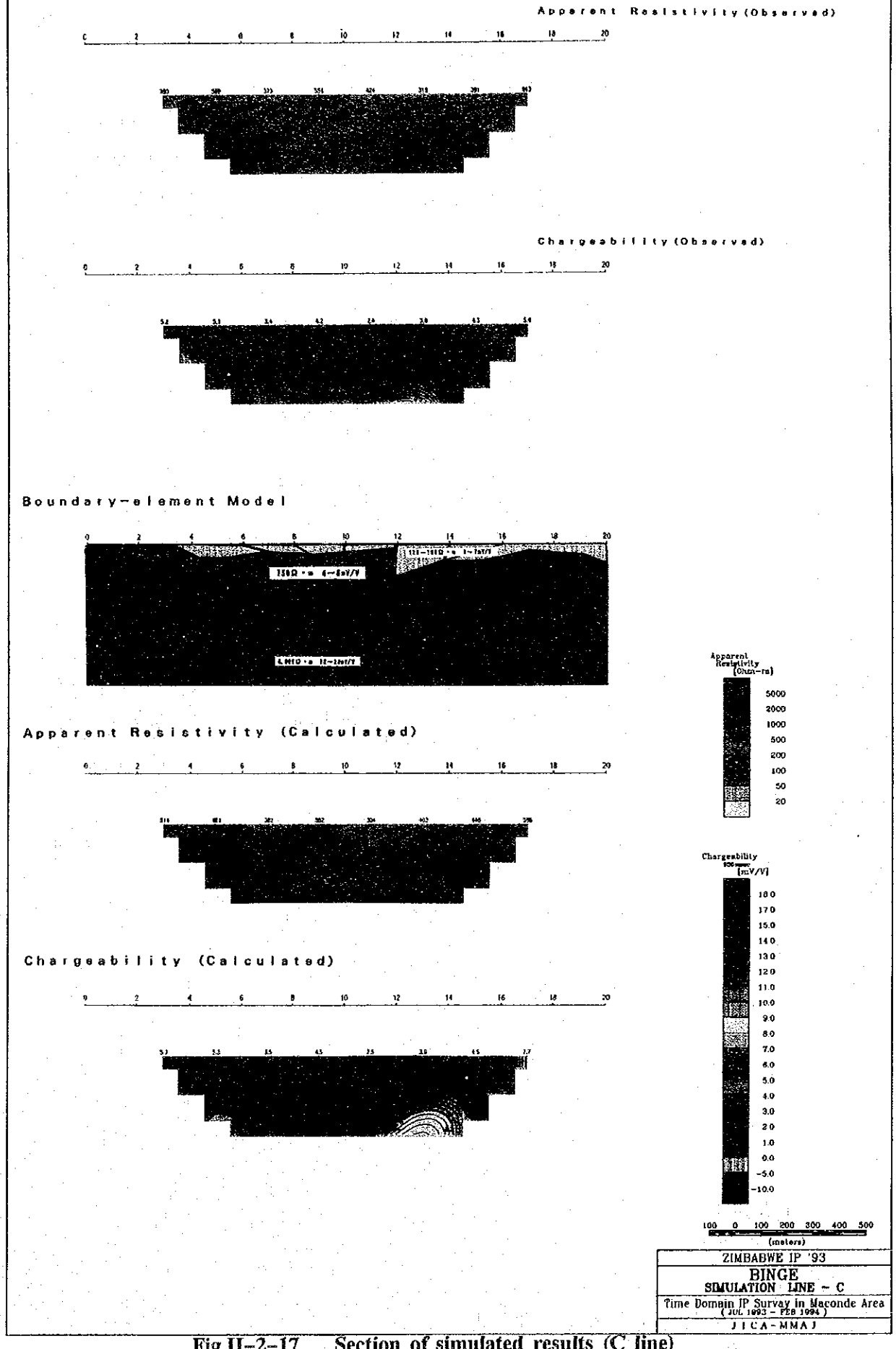

Fig.II-2-17 Section of simulated results (C line)

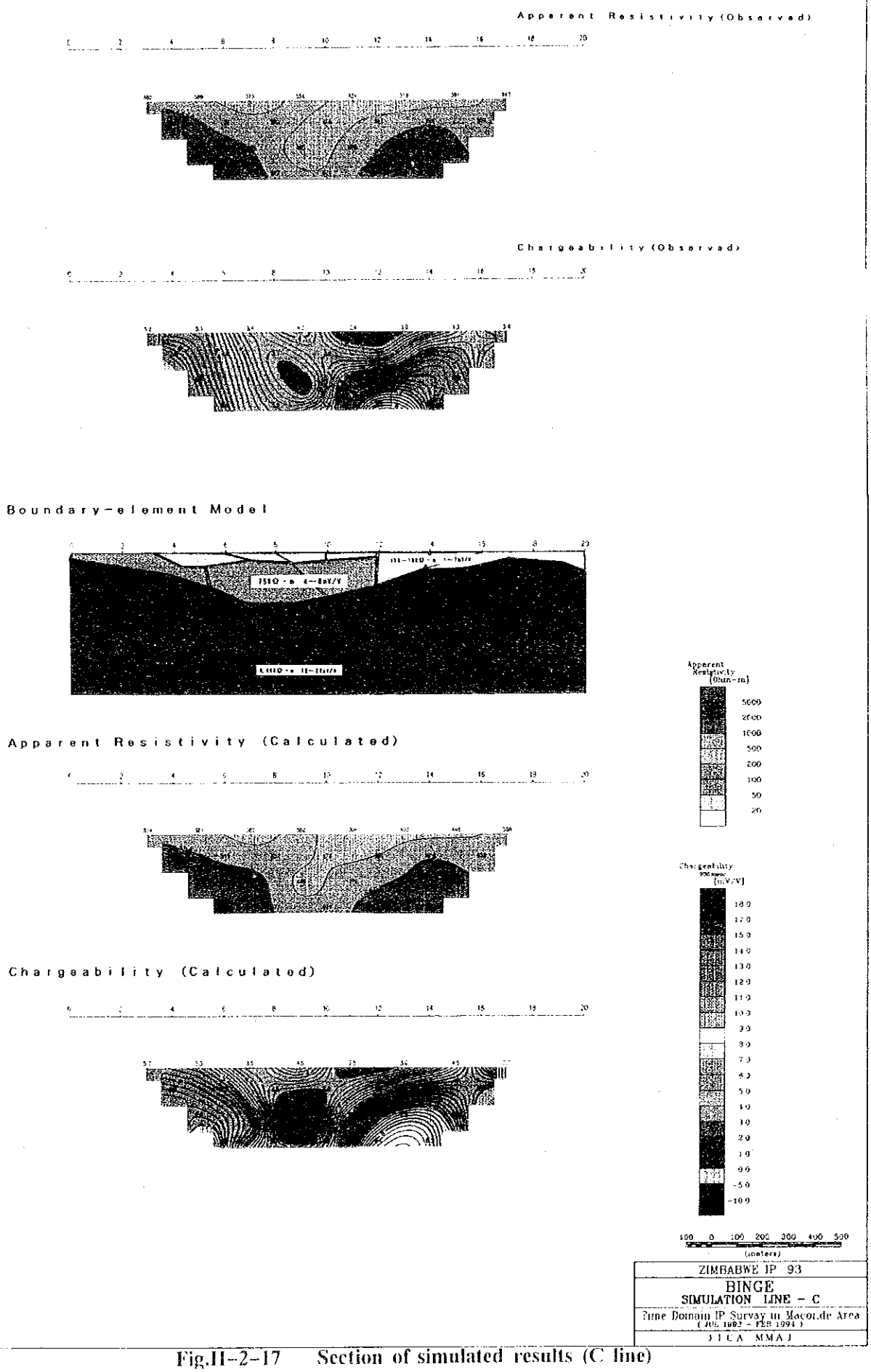

Fig.II-2-17 Section of simulated results (C line)

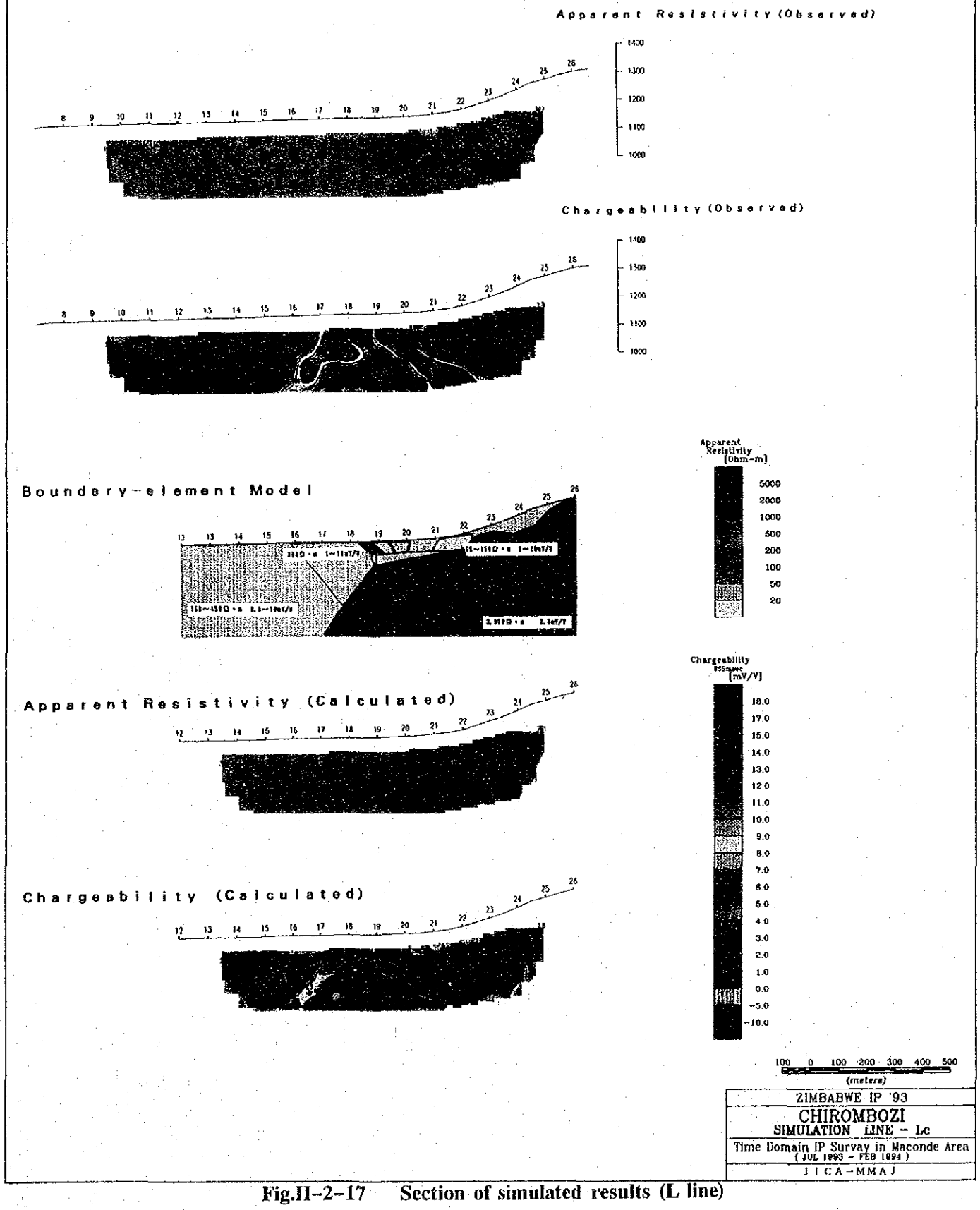

Fig.II-2-17 Section of simulated results (L line)

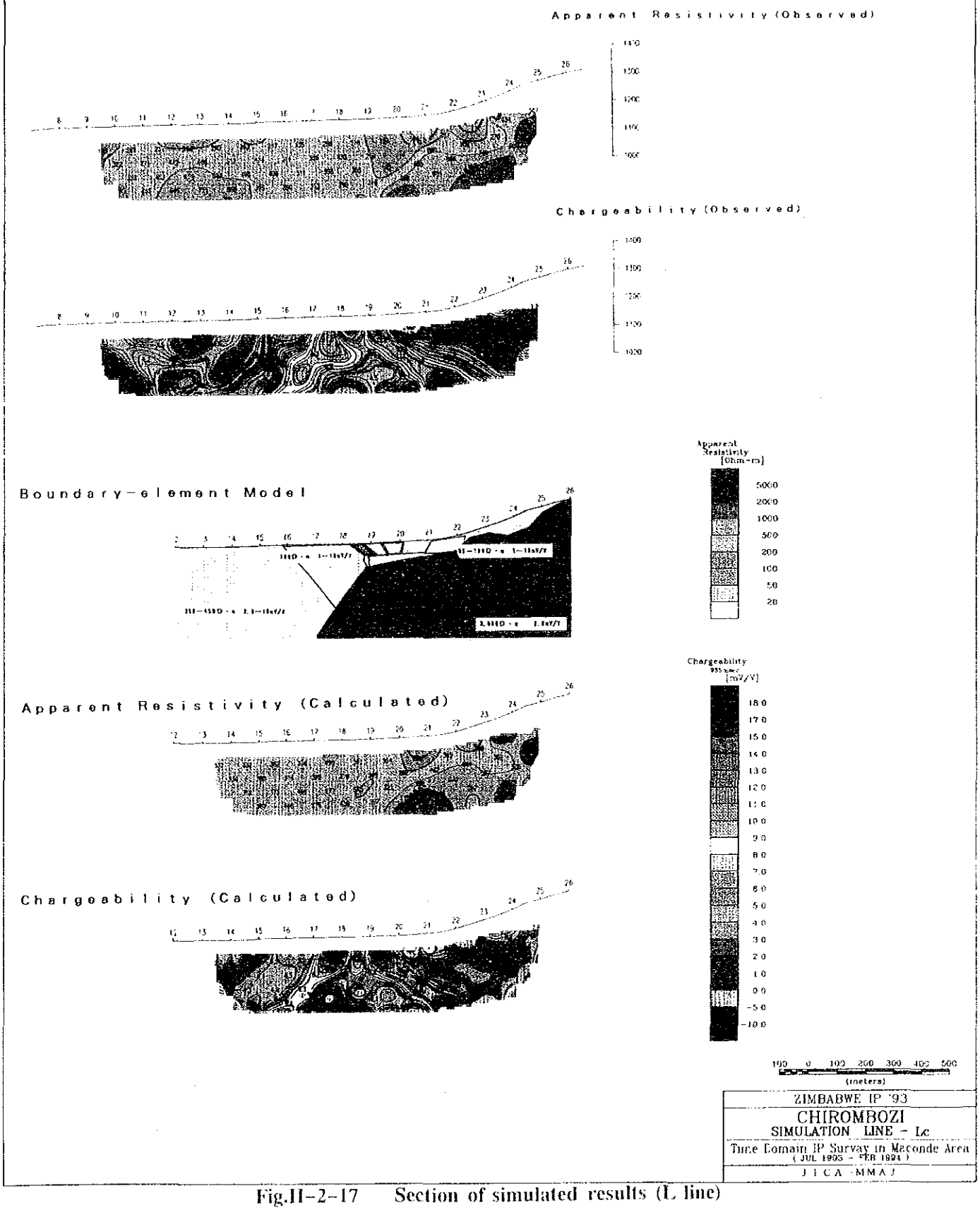

Fig.II-2-17 Section of simulated results (L line)

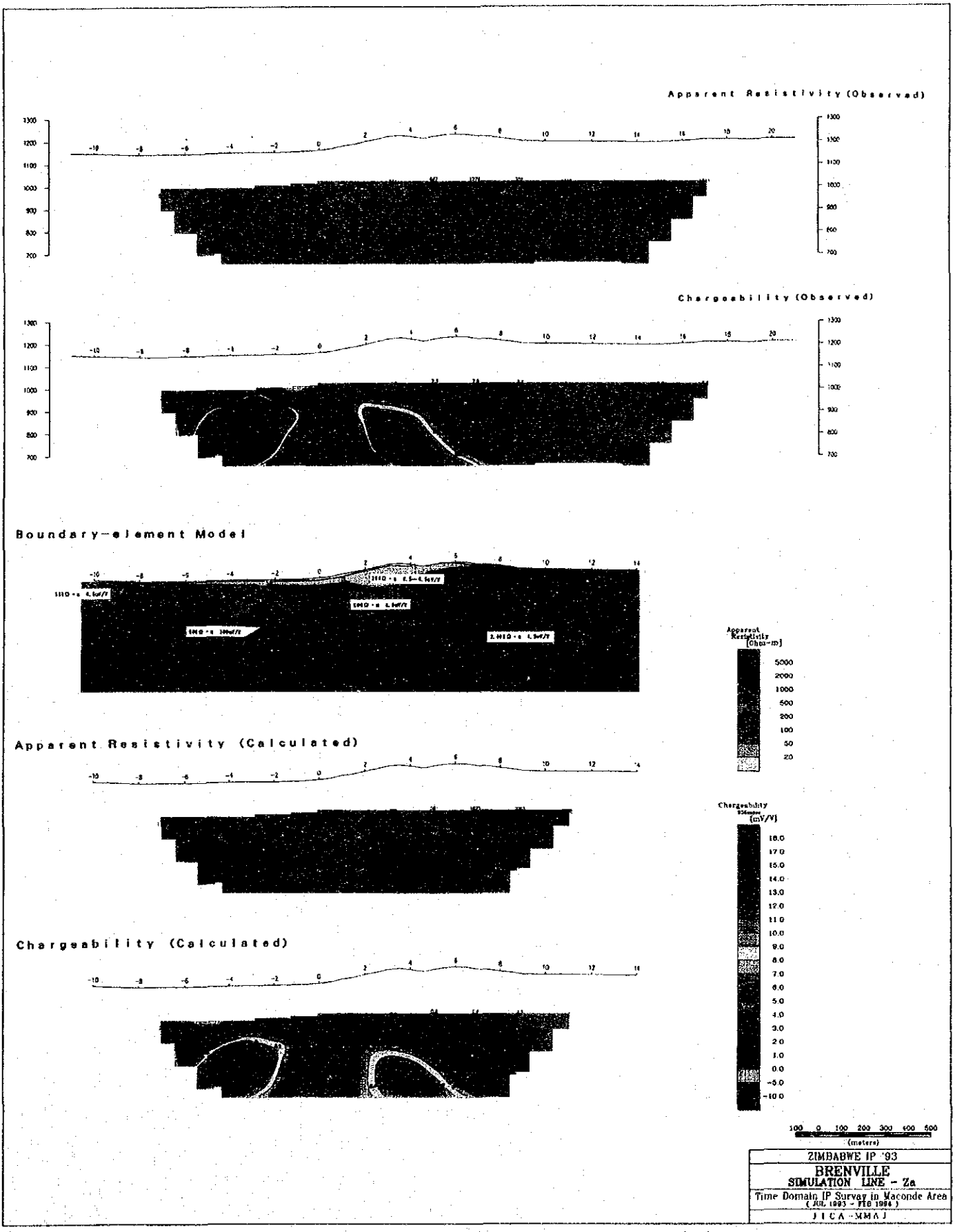

Fig.II-2-17 Section of simulated results (Za line)

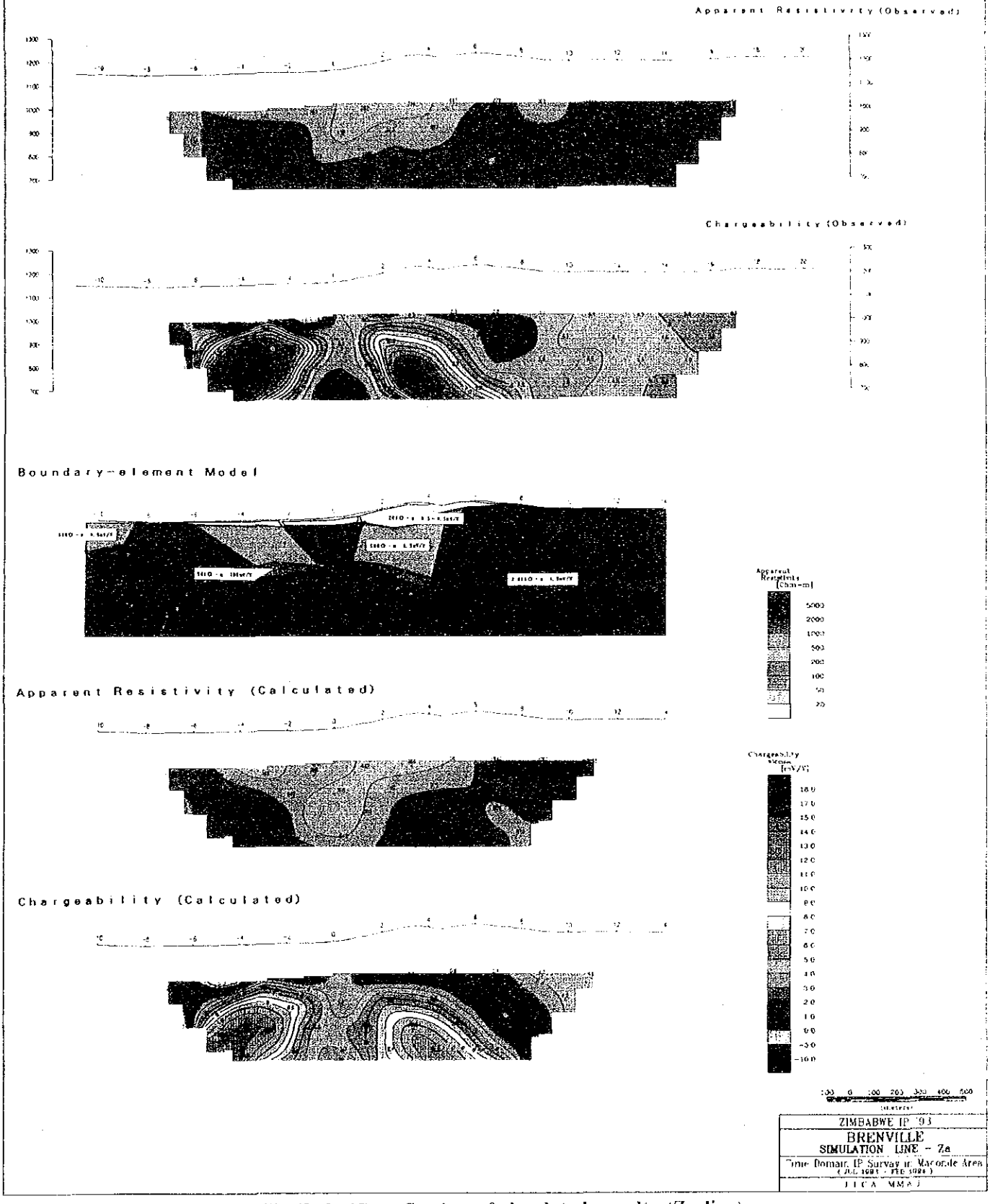

Fig.II-2-17 Section of simulated results (Za line)

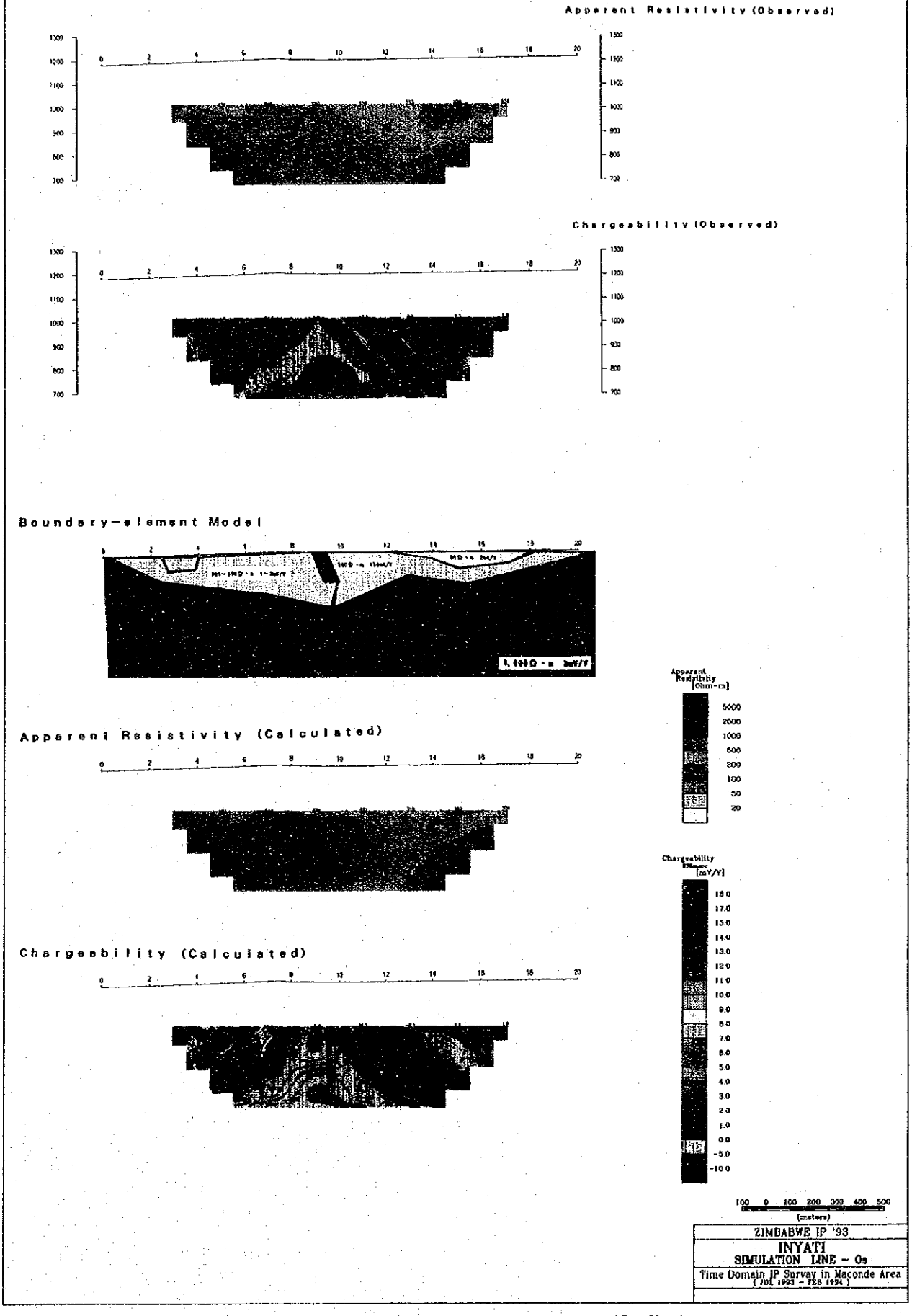

Fig.II-2-17 Section of simulated results (Os line)

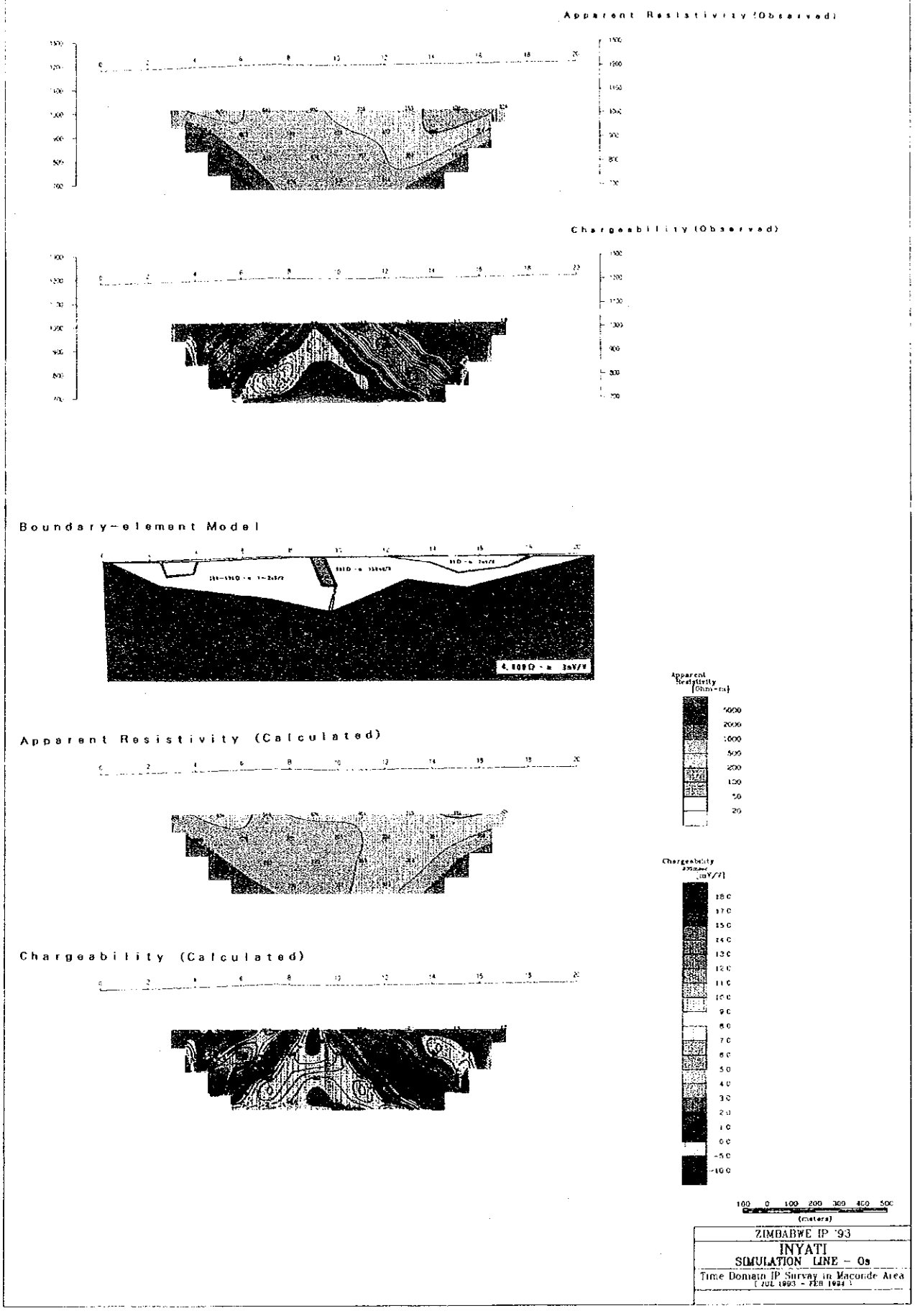

Fig.II-2-17 Section of simulated results (Os line)

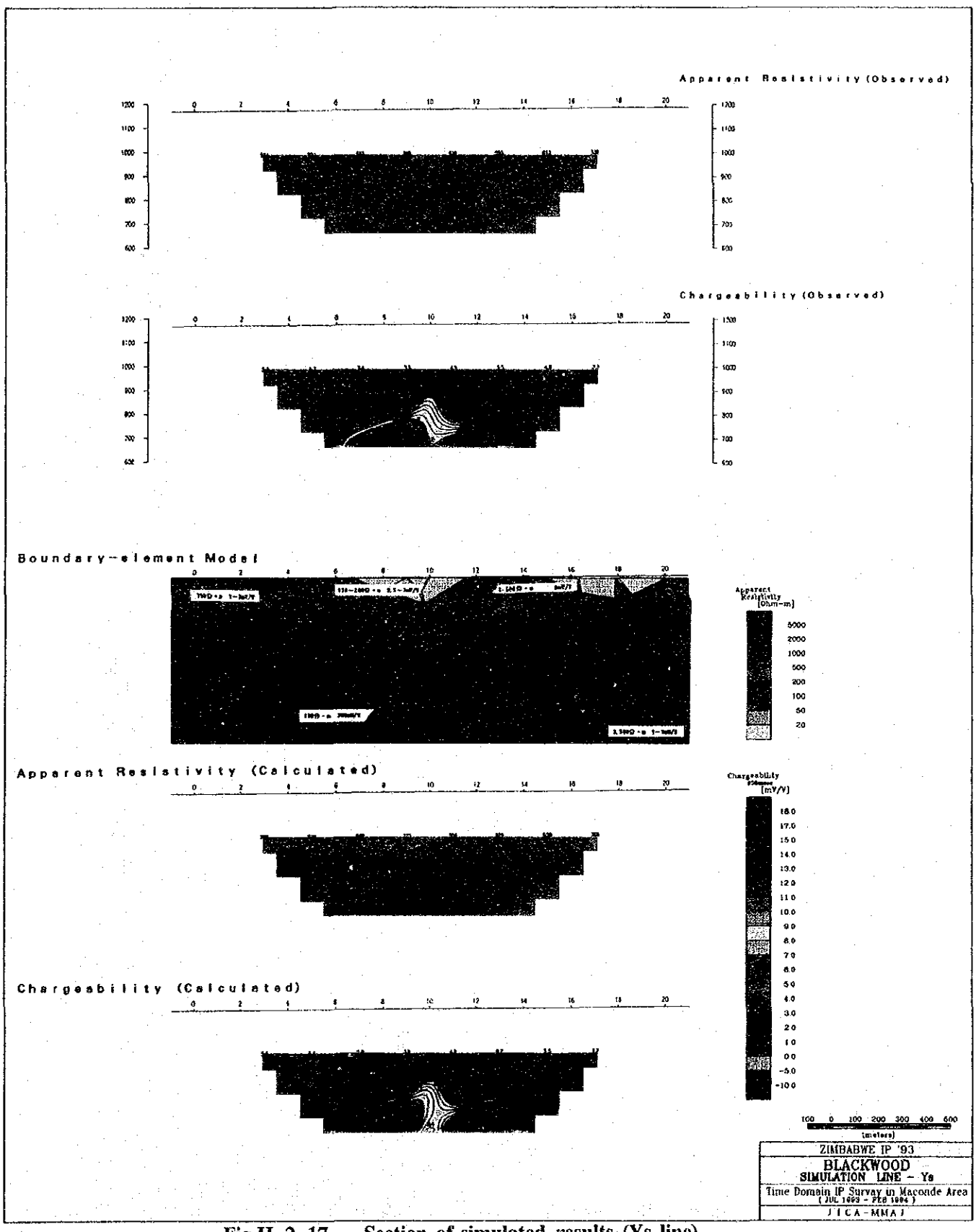

Fig.II-2-17 Section of simulated results (Ys line)

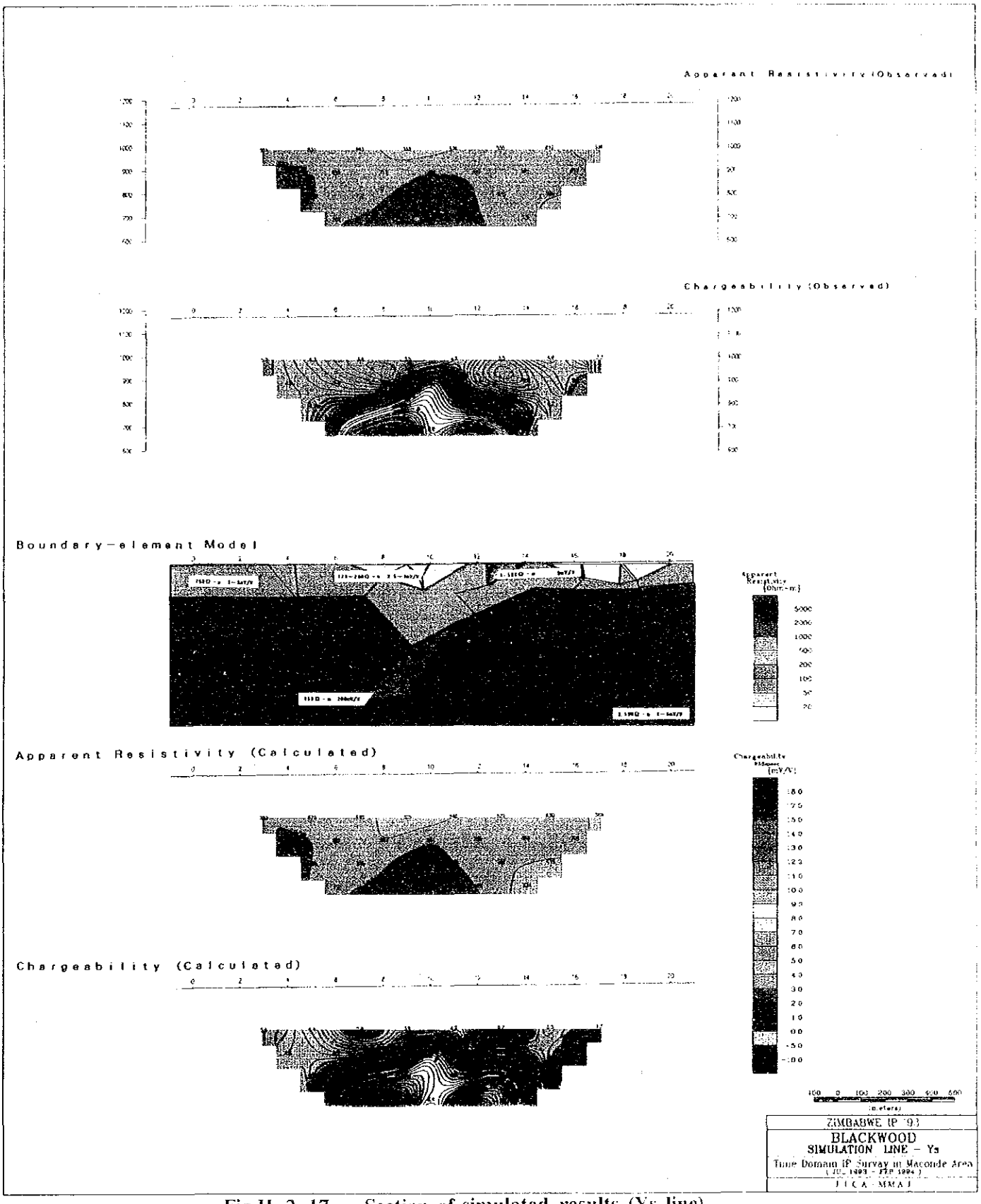

Fig.II-2-17 Section of simulated results (Ys line)

There are characteristically two kinds of high IP anomalous zones with low resistivity and high resistivity. High IP/low resistivity zones are distributed in B, O and L survey lines, and high IP/high resistivity zones are distributed in C, Za and Y survey lines.

On the other hand samples with sulphide mineralisation show a chargeability more than 10mV/V separated clearly from rock samples. Ores show low resistivity and high chargeability according to the extend of mineralisation, and in some cases show high chargeability of 100mV/V, high resistivity of 1,000Ω·m. Relationship between mineralisation and physical properties of low to high resistivity, high chargeability are evident.

Variety of resistivity of rock samples is due effect of extent of compaction and fine cracks in rocks.

Some samples show a variety of resistivity and chargeability, by the direction of transmition a electricity, simulation analysis might be affected by this physical property.

The IP anomalous zone in the stations No.0 to 10 of B survey line is geologically considered to reflect a mineralisation zone, because the IP anomaly is presumed to exist in the boundary area of slate,sandstone and arkose from the west to the east. By the results of simulation analysis, two different resistivity layers are presumed. The resistivity of the surface layer is low(25 to 300Ω·m) and that of the lower layer is high(3,000 Ω·m). Although the structure which is composed of such two layers is considered to be the anomalous pattern with two IP anomalies of the shallow and deep part of the underground, the IP anomaly is considered to reflect the graphitic slate of the western margin and the low IP of sandstone in the stations No.8 to No.10.

The IP anomaly in C survey line is located in the Pre-Magondi gneiss distribution area which is the virgin area for the survey of ore deposit. As a discovery of new ore deposit is expected, the pursuit of the eastern extension of the IP anomalous zone was tried by setting up the Cs survey line, however, an indistinct anomalous zone was detected.

The structure of resistivity distribution is considered to be composed of 130 to 180, 750 and 4,000 Ω·m resistivity zones in descending order by simulation analysis. IP anomaly pattern of the deep part is considered to reflect a high resistivity body(4,000 Ω·m, 20mV/V) which is widely distributed in the deep part.

IP anomalies in L(Lc) survey line are located in the shallow part and the deep part. The anomaly in the shallow part shows a distinct pattern. This IP anomaly is considered to reflect a small anomalous body(70mV/V) by simulation analysis. The existence of a small mineralisation zone is indicated by the geological condition, IP anomalous pattern and the peculiar value of the analysis.

Almost the same IP anomaly in the Lc survey line was detected in the Ln survey line. Although this anomalous zone suggests the continuation along the direction of strike from north to south, the IP value is low. This IP anomalous zone is presumed to be indistinct in the northern and the southern side of the L survey line.

An IP anomaly on a large scale with the centre near the station No.0 of Za survey line has been recognised.

This area is an arkose distribution area and granite is distributed in the eastern part of the station No.4.

The IP anomalous zone is also distributed in the geological strike of the Mhangura mine(working, 1km south).

This IP anomaly is presumed to be a flat shaped high IP anomalous body (300mV/V) by simulation analysis. The discovery of new ore deposit is expected in this area by geological condition, IP anomalous pattern and peculiar value of analysis.

IP anomalies with direction from north to south which is parallel to the strike of geology are recognised in the On, O, Os and Oss survey lines.These IP anomalies are considered to be similar to the United Kingdum ore deposit (work suspended) which is located 500m south of the Oss survey line.

The IP anomaly was analysed as a comparatively small body.

This IP anomalous body is considered to be a mineralisation zone by geological conditions, IP anomalous pattern and singularity(150mV/V), however, increase to the deeper part is not expected. Although the scale of the anomalous body is the largest in the Os survey line, the scale is presumed to be smaller in the north and the south side of the Os survey line.

As an IP anomaly was considered to be detected in the western end of the X survey line, survey lines Xn and Xs were newly set up. However, only indistinct IP anomalous patterns which reflect the small anomalous body in the shallow part were detected in these survey lines. These weak IP anomalies suggest the continuation in the direction of the south-west to north-east which corresponds to the direction of strike and intrusives. The existence of a mineralisation zone is considered possible, but the mineralisation zone is presumed to be very small.

Distinct high IP anomalies were detected in Y and Ys survey lines. The depth of the anomalous bodies become shallower to the south. The IP anomalies in each survey line were detected near the dolerite area which intruded north-east to south-west direction into arkose distribution area. The direction of this IP anomalous zone corresponds to the strike of the Hans(1,000m south) ore deposit and both of the geological situations are same. High IP anomaly in the deep part is considered to be the reflection of a mineralisation zone.

The flat shaped high IP anomalous body with an inclination to the west is presumed to be of a depth of more than 200m by simulation analysis.

Electric anisotoropy was shown in some rock and ore samples by measurement of physical properties, therefore, apparent resistivity and chargeability in the fields might be affected

complicatedly by these electric anisotropy. In addition, as in the case of measurement in L and Lc survey lines, sensitivity for expected anomalous body was decreased by smoothing according to be longer the distance of electrodes. The existence of mineralisation zones are expected in the IP anomalous zones detected in the L, Za, O, Os, Oss, Y and Ys survey lines, however, it is important to be careful about estimating the IP anomalous bodies by simulation analyses.

Distribution of IP anomalous body are shown Fig.II-2-18.

Although weak IP anomalies were detected in I, Q, R and S survey lines, they are possibly a part of high IP anomalies. As the target of this year's survey was Cu anomalies near the surface, the mineralisation zones which are located in the deeper part were not detectable. Therefore, a further survey for the possible deeper mineralisation zone will be necessary in the above survey lines.

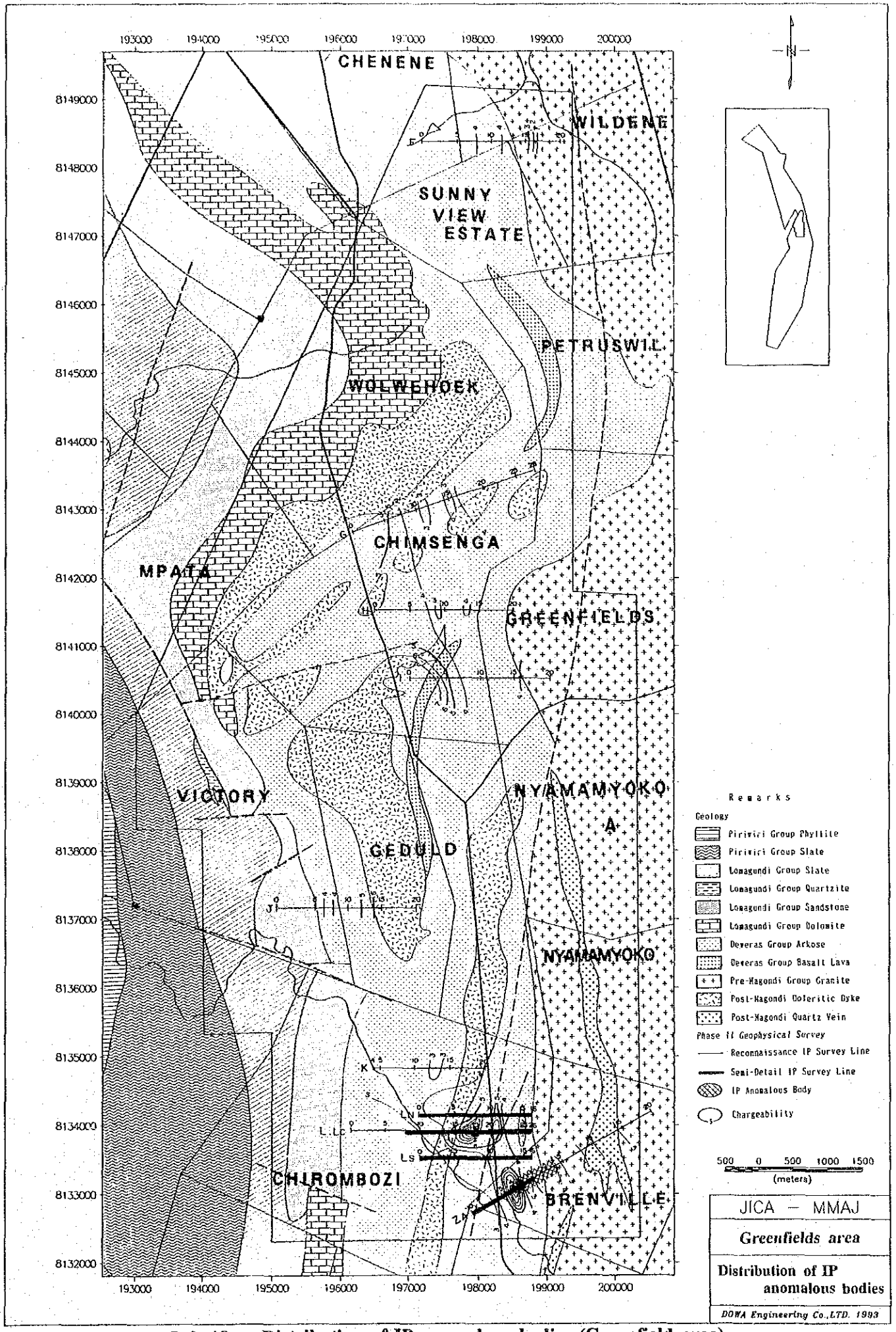

Fig.II-2-18 Distribution of IP anomalous bodies (Greenfield area)

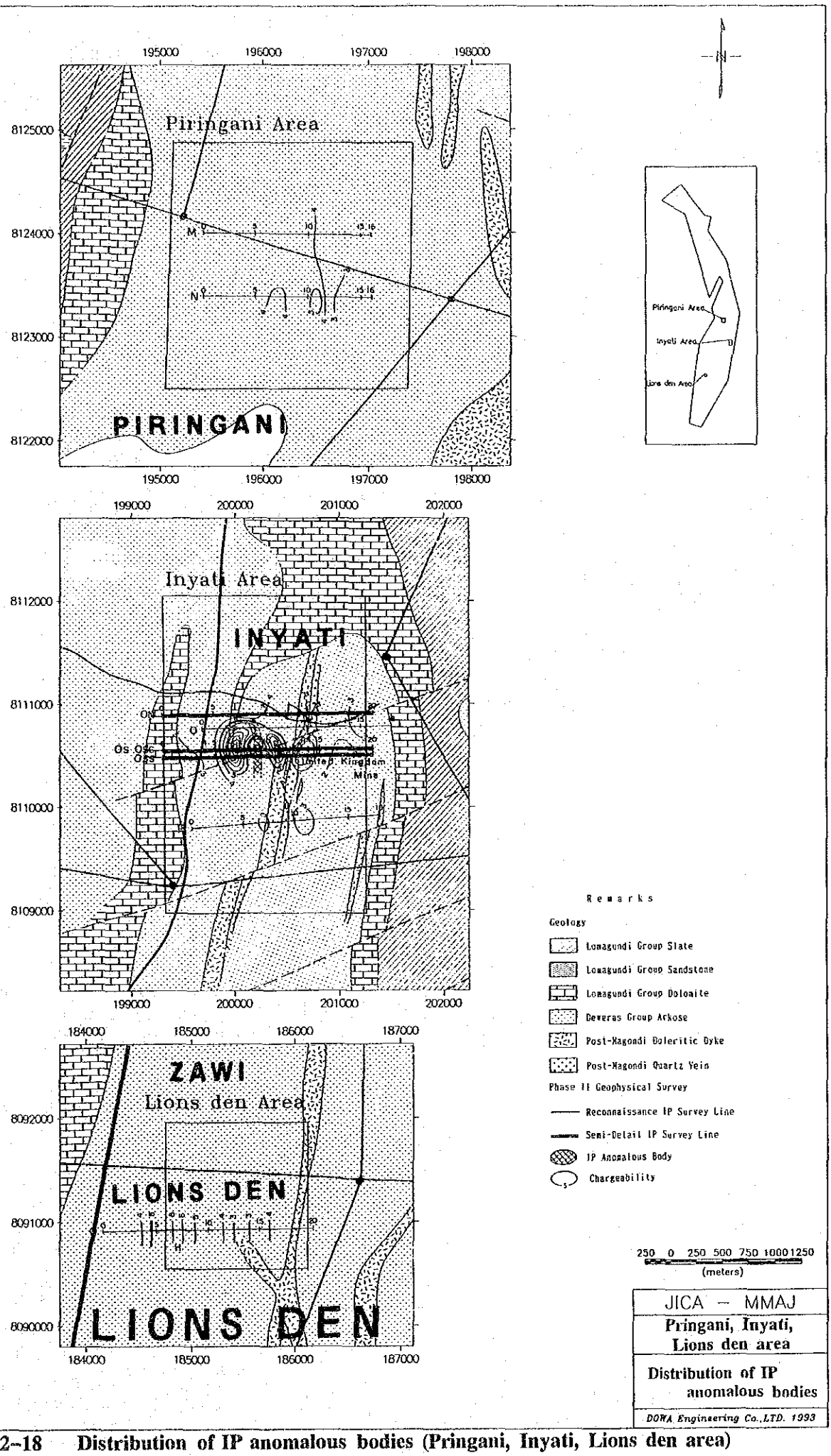

Fig.II-2-18 Distribution of IP anomalous bodies (Pringani, Inyati, Lions den area)

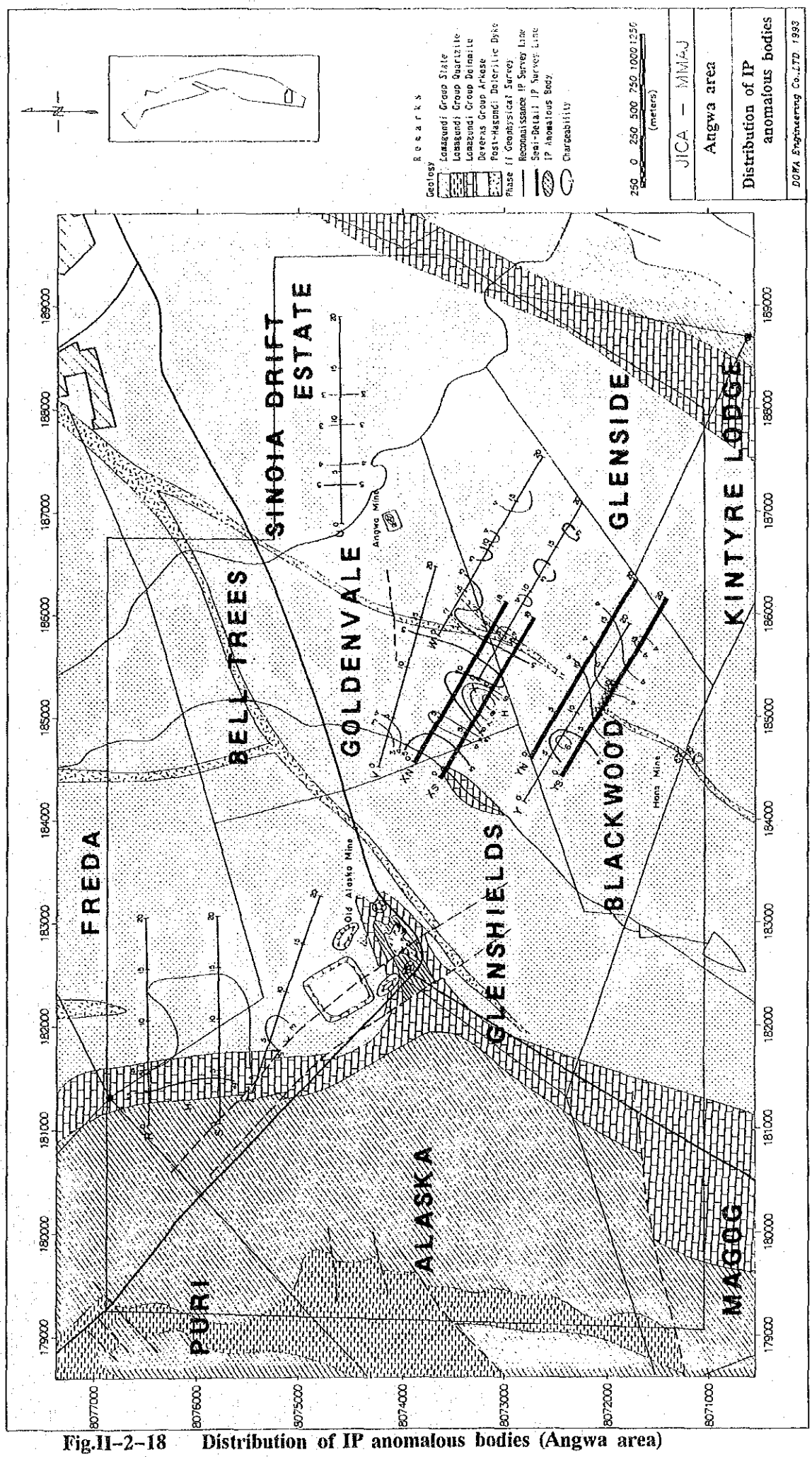

Fig.II-2-18 Distribution of IP anomalous bodies (Angwa area)